February 6, 1984

Dr. Michael Stroscio
AFOSR/NP
Bolling AFB
D. C. 20332

Reference: Grant AF AFOSR82-0241 , Final Scientific Report
'Numerical and Analytical Studies of Steady Detonation Waves with Expansion Losses.'
P. I. Dr. Manuel A. Huerta
University of Miami, Department of Physics.

Attached please find the Final Report for the referenced Grant. The grant had a budget of $29,186 and supported 3 months of work. The effort was concentrated on numerical solutions of the steady detonation equations with a model expansion loss. The aim was to find multiple propagation speeds and detonation failure. Some interesting results were found.

I would like to express my appreciation for the support I received under this grant.

Sincerely

Manuel A. Huerta

Manuel A. Huerta
Professor of Physics

UNCLASSIFIED

SECURITY CLASSIFICATION OF THIS PAGE

REPORT DOCUMENTATION PAGE

1a. REPORT SECURITY CLASSIFICATION: Unclassified	1b. RESTRICTIVE MARKINGS
2a. SECURITY CLASSIFICATION AUTHORITY	3. DISTRIBUTION/AVAILABILITY OF REPORT: Approved for public release; distribution unlimited
2b. DECLASSIFICATION/DOWNGRADING SCHEDULE	
4. PERFORMING ORGANIZATION REPORT NUMBER(S)	5. MONITORING ORGANIZATION REPORT NUMBER(S): AFOSR-TR- 84-0160
6a. NAME OF PERFORMING ORGANIZATION: University of Miami; 6b. OFFICE SYMBOL (If applicable)	7a. NAME OF MONITORING ORGANIZATION: AFOSR
6c. ADDRESS (City, State and ZIP Code): Department of Physics, Coral Gables, FL 33124	7b. ADDRESS (City, State and ZIP Code): Bldg 410, Bolling AFB, DC 20332
8a. NAME OF FUNDING/SPONSORING ORGANIZATION: AFOSR; 8b. OFFICE SYMBOL (If applicable): NP	9. PROCUREMENT INSTRUMENT IDENTIFICATION NUMBER: AFOSR-82-0021
8c. ADDRESS (City, State and ZIP Code): Bolling AFB, DC 20332	10. SOURCE OF FUNDING NOS. PROGRAM ELEMENT NO. 2308 PROJECT NO. A1 TASK NO. B6 WORK UNIT NO.

11. TITLE (Include Security Classification): NUMERICAL & ANALYTICAL STUDIES OF [illegible] WITH EXPANSION WAVES

12. PERSONAL AUTHOR(S): Dr. Manuel A. Huerta

13a. TYPE OF REPORT	13b. TIME COVERED	14. DATE OF REPORT (Yr., Mo., Day)	15. PAGE COUNT
FINAL	FROM 1 Jul 82 TO 30 Jun 84	84	49

16. SUPPLEMENTARY NOTATION

17. COSATI CODES: FIELD	GROUP	SUB GR	18. SUBJECT TERMS (Continue on reverse if necessary and identify by block number)

19. ABSTRACT (Continue on reverse if necessary and identify by block number)

The differential equations for the evolution of the fluid quantities in steady detonation waves are integrated numerically using a fourth order Runge-Kutta-Fehlberg method. Strong and weak detonation waves are found as well as detonation failure. In the weak regime there is a continuum of propagation speeds for a given expansion loss.

84 06 28 010

20. DISTRIBUTION/AVAILABILITY OF ABSTRACT: UNCLASSIFIED/UNLIMITED [illegible]	21. ABSTRACT SECURITY CLASSIFICATION: Unclassified
22a. NAME OF RESPONSIBLE INDIVIDUAL: Radoski	22b. TELEPHONE NUMBER (Include Area Code): (202) 767-4906
22c. OFFICE SYMBOL: NP	

DD FORM 1473, 83 APR — EDITION OF 1 JAN 73 IS OBSOLETE

SECURITY CLASSIFICATION OF THIS PAGE

FINAL SCIENTIFIC REPORT

AIR FORCE OFFICE OF SCIENTIFIC RESEARCH

GRANT NUMBER AF AFOSR82-0241

'Numerical and Analytical Studies of Steady Detonation Waves with Expansion Losses'

Principal Investigator: Dr. Manuel A. Huerta
Department of Physics
University of Miami
Coral Gables, Florida 33124

ABSTRACT

The differential equations for the evolution of the fluid quantities in steady detonation waves are integrated numerically using a fourth order Runge-Kutta-Fehlberg method. Strong and Weak detonation waves are found as well as detonation failure. In the weak regime there is a continuum of propagation speeds for a given expansion loss.

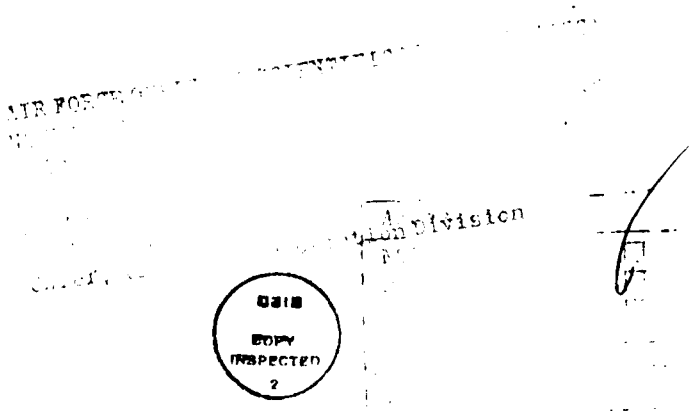

INTRODUCTION

To avoid repetition the initial proposal for this grant is attached as an Appendix to this Final Report. The work in the grant was to study the existence of multiple propagation speeds and detonation failure for one dimensional steady detonation waves with expansion losses. The theoretical treatment was based on the model developed in Sec.5G of the book by Fickett and Davis[1]. Only the steady reaction region between the initiating shock front and the sonic locus was considered. The main fluid quantities are the Mach number squared, $m = u^2/c^2$, and the reaction progress variable, λ. These quantities obey the equations

$$\frac{2(1-m)dm/dx}{m(1+\gamma m)(2+(\gamma-1)m)} = \frac{d(\sum \lambda_i q_i)/dx}{\sum \lambda_i q_i + H_1 + u_1^2/2} - \frac{2\varepsilon}{1+\gamma m} \quad , \qquad (1)$$

$$\frac{d\lambda_i}{dx} = \frac{R_i}{u} \quad , \qquad (2)$$

and

$$c^2 = \frac{2(\gamma-1)}{2+(\gamma-1)m} \left(\sum \lambda_i q_i + H_1 + u_1^2/2\right) \quad .$$

The losses are taken into account by the parameter ε as defined in the proposal. In reality the expansion loss is not a given quantity. It is determined by the complete three dimensional flow of the explosive charge and the confining medium. This entails solving a free boundary problem of great complexity. The chemical reaction rate R_i is given in Eq.(3) of the proposal. It involves the parameters B and G and RV that appear in the figures below. G is merely the ratio of the specific heats, γ, while B and RV characterize

the strength of the explosive. B was defined in the proposal, and RV is given by $RV = c_o^2/2q$. The larger the heat of reaction, q, that is released, the smaller B and RV are. However, B increases with the activation temperature of the reaction.

We are in the frame of the reaction front. The unreacted explosive fluid approaches from $x < 0$ with a supersonic detonation velocity D to be determined. D will be obtained in terms of the Mach number squared $m_o = D^2/c_o^2 > 1$ in front of the shock at $x = 0^-$. The flow at $x=0^+$, immediately behind the shock, is subsonic. The Mach number squared $m_1 = (u_1/c_1)^2$ at $x = 0^+$ satisfies $m_1 \leq 1$ and is related to m_o by the usual Hugoniot relations[2]

$$m_1 = \frac{2 + (\gamma-1)m_o}{2\gamma m_o - (\gamma-1)} ,$$

and

$$c_1^2 = c_o^2 \frac{(2\gamma m_o-(\gamma-1))(2+(\gamma-1)m_o)}{m_o(\gamma+1)^2} .$$

Several authors have considered this model with different reaction rates R_i and expansion loss terms ε. Wecken[3] considered the case ε = constant and obtained partial results on multiple solutions and detonation failure. Tsuge[4] et al., and Fujiwara and Tsuge[5] have integrated the nozzle equations numerically for a hydrogen/oxygen detonation with a good model for the lateral expansion. They have shown that sufficiently great expansion losses lead to detonation failure. They also obtain two detonation speeds that join at the failure diameter. For small losses the fast root goes to the Chapman-Jouguet value. They conjectured that the slow root went to Mach one as the losses

decreased to zero (charge diameter$\longrightarrow \infty$). They were not able to verify it due to the large amounts of computer time required.

METHOD OF SOLUTION

The phase plane of Eqs.(1) and (2) is extraordinarily complex even with ε = constant as we take it here. Let $F(m, \lambda ; m_o, \varepsilon)$ be the right hand side of Eq.(1) so the curve $F = 0$ (with m_o and ε fixed) is the same as the locus of $dm/d\lambda = 0$ in the $m - \lambda$ plane. The singular points of Eqs.(1) and (2) are given by the intersections of the line $m = 1$ with the curve $F = 0$. The phase trajectory of the physical solution begins at the point immediately behind the shock where $x = 0^+$. There $\lambda = 0$ while m has the so far unknown value $m = m_1$. The crucial point is that the physical trajectory has to be transonic, that is it must cross the line $m = 1$ with a finite slope $dm/d\lambda$ so it can be joined to the rear flow behind the sonic point. Therefore the transonic trajectory has to cross the line $m = 1$ at a critical point. In normal phase plane problems the orbits may only go to the critical points asymptotically, reaching them only after an infinite distance (or time). Here the transonic trajectories do pass through the critical points due to the singularity at $m = 1$. The condition that the solution must be transonic is what determines the value of m_1 (as well as m_o which is related to m_1 by the Hugoniot relation). The curve $F = 0$ is not very complicated qualitatively. For different values in the physical range $(\gamma-1)/2\gamma < m_1 \leq 1$, the curve $F = 0$ intersects the line $m = 1$ a different number of times depending on the values of ε and m_o. In the cases considered here they can intersect twice, once, or not at all. The difficulty is that the curve $dm/d\lambda = 0$, and consequently the nature and position of the critical points, as well as the phase trajectories, depend on the unknown m_o(or m_1) that enters not only as an

initial value, but also as a parameter in the equations.

A typical case for a strong detonation solution is shown in Fig.1 where ε, as well as the parameters B, G, and RV are given in the table next to the figure. The curves $F = 0$ and $m = 1$ are shown in Fig.1. The curve $F = 0$ is computed numerically using a root finding algorithm (Derpar).In Fig.(1), the curve $F = 0$ is plotted for the value $m_o = 39.16$. The differential equations for the trajectories are integrated using a fourth order Runge-Kutta-Fehlberg method whose variable step size allows important savings in computer time. For $m_o = 37.16$ the phase trajectory starts at the point ($\lambda = 0$, $m_1 = 0.3454$) and reaches the line $m = 1$ with a vertical slope. This is a trajectory of type 2, a choking trajectory. For $m_o = 41.16$ the trajectory starts at ($\lambda = 0$, $m_1 = 0.3442$), crosses the line $F = 0$ and acquires a negative slope. This a trajectory of type 1, a subsonic trajectory. The transonic trajectory will have a value of m_o bracketed 37.16(type 2) < (transonic) < 41.16(type 1) ($m_o = 39.16$ is pretty close). It passes through the critical point at $m = 1$, $F = 0$. This is the sonic point. The problem of finding m_o is not an initial value problem, but rather a sort of boundary value problem. Its form is suitable for a Nonlinear Shooting Method[6]. We start with a value of m_o and get its trajectory. Then we change the value of m_o until the type of the trajectory changes. We have then bracketed the desired value of m_o. This procedure is done for each value of ε. In the end we produce a plot of m_o vs. ε that shows how the steady detonation speed varies with the loss parameter.

STRONG SOLUTIONS THROUGH HYPERBOLIC (SADDLE) CRITICAL POINTS

When the sonic point is a hyperbolic critical point (saddle point) the shooting method works well because there is a separatrix that separates the

trajectories of types 1 and 2 unambiguously. In fact, the transonic trajectory lies on the séparatrix. In all the cases considered here the singular point is hyperbolic if the curve F = 0 has a negative slope at the critical point (whenever we speak of a critical point it must be remembered that its position depends on m_o, so that as we vary m_o to produce different trajectories we are also moving the critical point). The phase trajectories of strong detonation waves always end at a saddle point. Fig.1 is a typical example of this situation. In general there is a range of values of ε where for each given ε one can find a single value of m_o (and therefore a single steady detonation speed) that yields a transonic trajectory and solves the problem. In the range of strong detonations m_o is a decreasing function of ε.

STRONG AND WEAK SOLUTIONS AND DETONATION FAILURE

There is another range of ε where there are two detonations speeds. That is, for a given ε there are two values of m_o that yield transonic trajectories through their respective saddle points. The solution with the larger value of $m = m_s$ is a strong detonation wave and the solution with the smaller m_w is a weak detonation wave. As ε increases, m_s decreases while m_w increases. An example is given in Figs.(2) and (3). The values of ε = 0.06, B = 6.83, G =3.0, and RV = 0.102 are the same in both figures. In the figures, the notation $F(m_o) = 0$ means that the curve is shown for the given value of m_o with the other parameters as given in the accompanying table. The value of m_o for the strong transonic trajectory in Fig.(2) is bracketed 21.57 (type 2) $< m_s <$ 23.57 (type 1). The value $m_s \approx 22.57$ is bracketed numerically much more closely than shown above. Those bracketing values are chosen for clarity in the figure. The strong detonation of Fig.(2) has the same type of bracketing as the case of Fig.(1), that is the transonic value of m_o is

bounded on the low side by a type 2 solution and on the high side by a type 1 solution. Fig.(3) shows a representative weak detonation case. The transonic value is bracketed by 13.0 (type 1) $< m_w <$ 15.0 (type 2). This bracketing for the weak solution $m_w \approx 14.06$ is the reverse of the strong one because the lower m_o value is type 1 while for the strong case the lower value was type 2. This is a distinguishing feature of the strong and weak solutions. Note that the curve F = 0 in both Figs.(2) and (3) looks pretty much like it did in Fig.(1). In each case there is just one saddle point. As ε increases, the weak and the strong solutions approach each other until they meet at $m_o = m_{df} \approx 17.08$ when $\varepsilon = \varepsilon_{df} \approx 0.0657$. After ε exceeds this value there is no transonic trajectory at all. This point is usually called detonation failure. Fig.(4) shows what the phase trajectories and the F = 0 curves look like just past that point, say for $\varepsilon = .08$. Past the detonation failure value the trajectories remain of type 1 as m_o is varied, no bracketing occurs, and there is no steady detonation solution. Note that there is still a saddle point in the range of m_o shown but it is not reached. One might have thought that detonation failure would only occur when the F = 0 curve stays so low that it never crosses the m = 1 line and there is no critical point. The actual limiting point of detonation failure does not occur when the F = 0 curve is tangent to the m = 1 line. It is a little more subtle than that.

The bracketings mentioned above are indicative of the behavior of the phase trajectories in the regions of strong and weak solutions. In the strong region the type 1 trajectories move higher monotonically as m_o is decreased. Then as one decreases m_o the trajectory rises until it becomes type 2 and the transonic value is bracketed. In the weak region the reverse happens. The type 1 trajectory moves higher monotonically as m_o is increased (rather than decreased) until it becomes type 2 and brackets the transonic trajectory.

Fig.(5) is a schematic that helps to visualize what is happening. Detonation failure occurs when these two behaviors interfere with each other so the trajectories do not behave monotonically with m_o. As we decrease m_o, raising the type 1 trajectory and expecting to reach a strong solution, the behavior reverses and the type 1 trajectory begins to move lower with further decreases in m_o as it does in the weak region. Consequently, the critical point is not reached and no transonic trajectory is found. This is evident in Fig.(4). Toward the left the trajectories are ordered in the strong way with 45 below 30 below 15. Far to the right they are ordered in the weak way with 15 below 30 below 45. In the region where the trajectories are crossing their order is not monotonic. This is what signals the proximity of the limiting point of detonation failure. Note also how the F = 0 curves reverse their ordering in this neighborhood.

The above discussion can be stated in a mathematically more precise way. In a phase trajectory of type 1, the function $m(\lambda)$ reaches its highest value at the point where the trajectory crosses the curve F = 0 (for type 2 trajectories it is more useful to consider the function $\lambda(m)$). Call this value $m_h(m_o,\varepsilon)$ noting that it is a function of the values of m_o and ε for that trajectory (unfortunately, this function is only known numerically). In the strong region $\partial m_h/\partial m_o < 0$, while in the weak region $\partial m_h/\partial m_o > 0$. Fig.(6) shows schematically the types of behavior of m_h vs. m_o for several fixed values of ε. In Fig.(6a) ε is in the double root region. Here m_s is the strong root and m_w is the weak root. In Fig.(6b) we are at the point of detonation failure where $\varepsilon = \varepsilon_{df}$. For that value $m_w = m_s$ and the $m_h(m_o,\varepsilon_{df})$ curve is tangent to the m = 1 line. In Fig.(6c) we are in the failed region, $\varepsilon > \varepsilon_{df}$ and there is no root.

CONTINUUM OF SOLUTIONS THROUGH A STABLE NODE

Another type of solution can occur when there are two sonic points. The curve $F = 0$ depends on both ε and m_o. As ε increases (or m_o decreases) the left side of the $F = 0$ curve bends down and may go below the $m = 1$ line. Then there are two singular points. The one with the larger value of λ is a saddle but the one with the smaller value of λ is a stable node (sink) in all the cases considered here. The stable node does not have a separatrix like the saddle point does. Rather it has limiting curves that act as edges for a continuum of type 3 trajectories. The type 3 trajectories are transonic. They pass through the stable node with a finite slope. The behavior is that for a given ε there is a continuous range of m_o values that yield type 3 trajectories. Values of m_o above the upper limit of the type 3 continuum yield trajectories of type 2. Values of m_o below the lower limit of the type 3 continuum may yield trajectories of type 1 or type 2 depending on what is happening with the coexisting saddle point. Therefore, we have two cases. The case $t2 < t3 < t2$, where the type 3 trajectories are bounded above and below by type 2 trajectories, and the case $t1 < t3 < t2$ where they are bounded below by type 1 trajectories and above by type 2. Fig.(7) shows an example of the behavior of the coexisting saddle point that will lead to the case $t2 < t3 < t2$. The parameters B, G, and RV are the same as in Figs.(2)-(4) and $\varepsilon = 0.0001$. Fig.(7) shows the $F = 0$ curve plotted for $m_o = 1.035$. The sink is to the left and the coexisting saddle point is far to the right. The transonic trajectory through the saddle point is bracketed 1.03 (type 1) $< m_{wbc} < 1.04$ (type 2). We call the transonic value here m_{wbc} because this is a weak root (note that type 1 brackets below) that lies below the continuum. As we increase m_o the type 1 trajectory rises and becomes type

2 around $m_o \approx 1.04$. We continue to increase m_o and the type 2 trajectory keeps rising, moving mostly to the left, and we enter the picture shown in Fig.(8). Here the lowest type 2 curve has $m_o = 1.25$. Increasing m_o produces higher type 2 curves, we just show the one for $m_o = 1.4$. Increasing m_o further gets us into the type 3 curves. They are shown here for $m_o = 1.7$, 2.2, 2.7, and 3.2 but there is a continuum of these transonic solutions. They have a characteristic shape. They reach the m = 1 line with a finite slope because they are all going through their respective sinks (recall that the singular point moves as we change m_o). Finally we pass the continuum of type 3 and run into type 2 curves again near $m_o \approx 3.7$. This case of t2 < t3 < t2 seems to be rare because it occurs here only in a narrow range of ε and does not occur at all in some of the other examples shown below where we take different values for B and RV. Fig.(9) shows the type 3 continuum in the case t1 < t3 < t2. The trajectory rises as we increase m_o. We start with type 1 at $m_o = 2.0$. The trajectory rises, but is still type 1 at 2.5. Near $m_o \approx 2.77$ (not shown) the type 3 trajectories start. We show type 3 trajectories for $m_o = 3.0$, 3.5, 4.0, 4.5, 5.0, and 5.5 but there is a continuum of transonic trajectories here going through their respective singular points. The continuum ends near $m_o \approx 5.5$ and we pass into type 2 curves. We show the ones for $m_o = 6.0$, and 6.5 (they lie almost on top of each other). In this t1 < t3 < t2 case we pass directly from type 1 to type 3 at the lower limit of the continuum. The weak saddle point (not shown in Fig.(9)) that lies far to the right of the node is not reached by any trajectory in this case. This is due to the behavior of the F = 0 curve and can be understood looking at Figs.(10) and (11).

In Fig.(10) the curve F = 0 is shown for $\varepsilon = 0.0025$ and $m_o = 2.5$. There are no singular points. Also shown is the type 1 trajectory for

$m_o = 2.5$. Note how the type 1 curve starts with a negative slope and goes under the F = 0 curve. Then it rises up to the F = 0 curve and looks like it would become a type 3 curve if only a sink were available. The type 1 curve then follows the F = 0 curve very closely until it finally gets above it and dips down as a type 1 trajectory is supposed to do. In Fig.(11) we show the F = 0 curve for $m_o = 3.5$, a little bigger than in Fig.(10). Now there are both a sink and a saddle point. What was a type 1 trajectory curve for $m_o = 2.5$ in Fig.(10) has evolved directly into a type 3 that closely follows the F = 0 curve until it hits the stable node. This explains the t1<t3 bracketing in the lower part of the continuum. The trajectories are trapped in the sink and cannot approach the region near the saddle point. In this situation the saddle point has little effect on the relevant flow regions of the phase flow.

SUMMARY OF RESEARCH RESULTS

The discussion above, illustrated by Figs.(1) - (11) covers all the qualitative features that were encountered. Fig.(12) shows the curve for the transonic values of m_o vs. ε for the parameters B = 12.5, G = 3.0, and RV = 0.41 . These parameter values, as well as the others used here are related to examples given in Ref.1. We only consider the detonation region, which lies above the line $m_o = 1$. The detonation part of the $\varepsilon - m_o$ plane is divided into 3 regions , labeled 1, 2, and 3. The label indicates what type of trajectory is produced by a pair (ε, m_o) that lies in that region. So, for example, if the pair (ε, m_o) lies in region 2 the trajectory associated with it is type 2.

The pairs (ε, m_o) that lie on the curves that separate the regions produce transonic trajectories bracketed by the two adjacent types of trajectories. Therefore the curves give the dependence of the speed of steady

detonation waves vs.the loss parameter. Region 3 is the continuum, so any point in that region gives a transonic trajectory of type 3. Fig.(13) has B and RV half as large as in Fig.(12). This represents an explosive with twice the heat of reaction as the first one but the same activation temperature. This is clearly a stronger explosive with larger detonation speeds but no qualitative differences. For both of these explosives there is a lack of the weak roots below the continuum so region 3 is bounded below by region 1 (or, of course by the $m_o = 1$ line).

Fig.(14) shows a case with the heat of reaction again doubled (RV is one fourth of the first example), but whose activation energy is twice as large as the other examples. For small losses, the detonation speed is larger (in all these cases it goes to the ideal Chapman-Jouguet value) than the others. This case exhibits the weak solutions below the continuum so the detonation part of the $\varepsilon - m_o$ plane is now divided into four regions. The region of type 2 below region 3 is hardly visible in Fig.(14). Fig.(15) is an expanded view that shows the small region. Another feature of this last example is how slowly the upper limit of region 3 goes to $m_o = 1$. In the previous two examples the continuum ends near $\varepsilon \approx 0.00001$. In this example the upper limit of the continuum extends to much smaller values of ε. The calculation of the trajectories in this neighborhood are the longest ones. What happens is that at these small values of m_o the reaction rate starts very small and the reaction requires a longer distance to develop. This is more pronounced the larger the activation temperature. Here we can have reaction zone thicknesses that are millions of times longer than they are in the strong detonation cases.

The physical significance of model calculations such as the one done in

this work is not clear. In real explosives the detonation speed is reduced when the losses are increased in agreement with the curves in Figs.(12) - (15). However, the limiting point of detonation failure sets in very early in real explosives, after the detonation speed has fallen only about 10 percent. In these examples, the limiting point of detonation failure occurs after m_o has dropped by 75 percent and more. Possibly the solutions of region 3 have an influence in producing a much earlier detonation failure. If the strong detonation wave were in a range of ε where the continuum exists, it might excite a lot of the weaker type 3 waves that would drain away the energy.

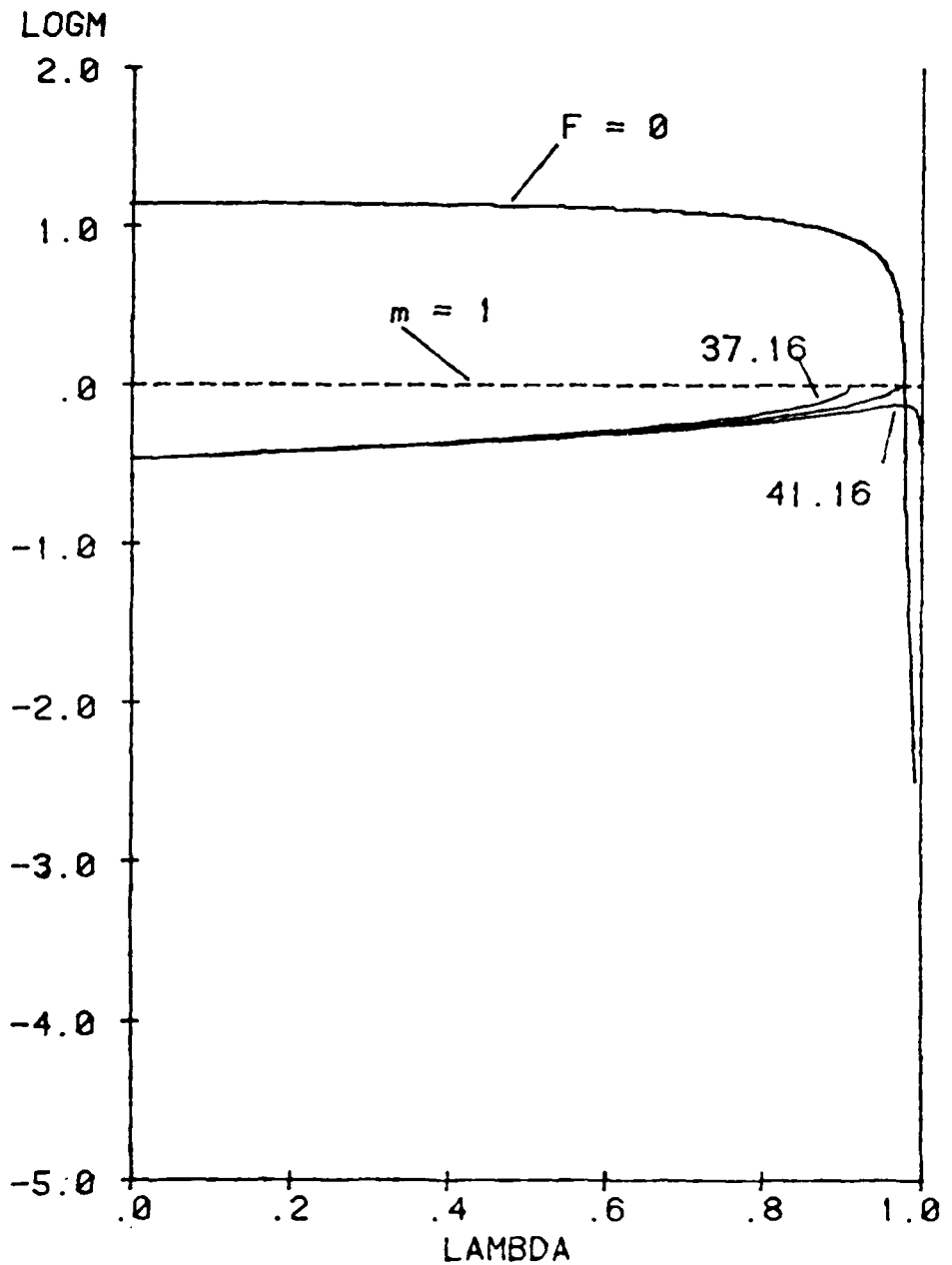

G=V= 3.000

B	RV	M0	EPSILO	TYPE
6.830	.205	37.160	.0001000	2
6.830	.205	39.160	.0001000	2
6.830	.205	41.160	.0001000	1

FIGURE 1

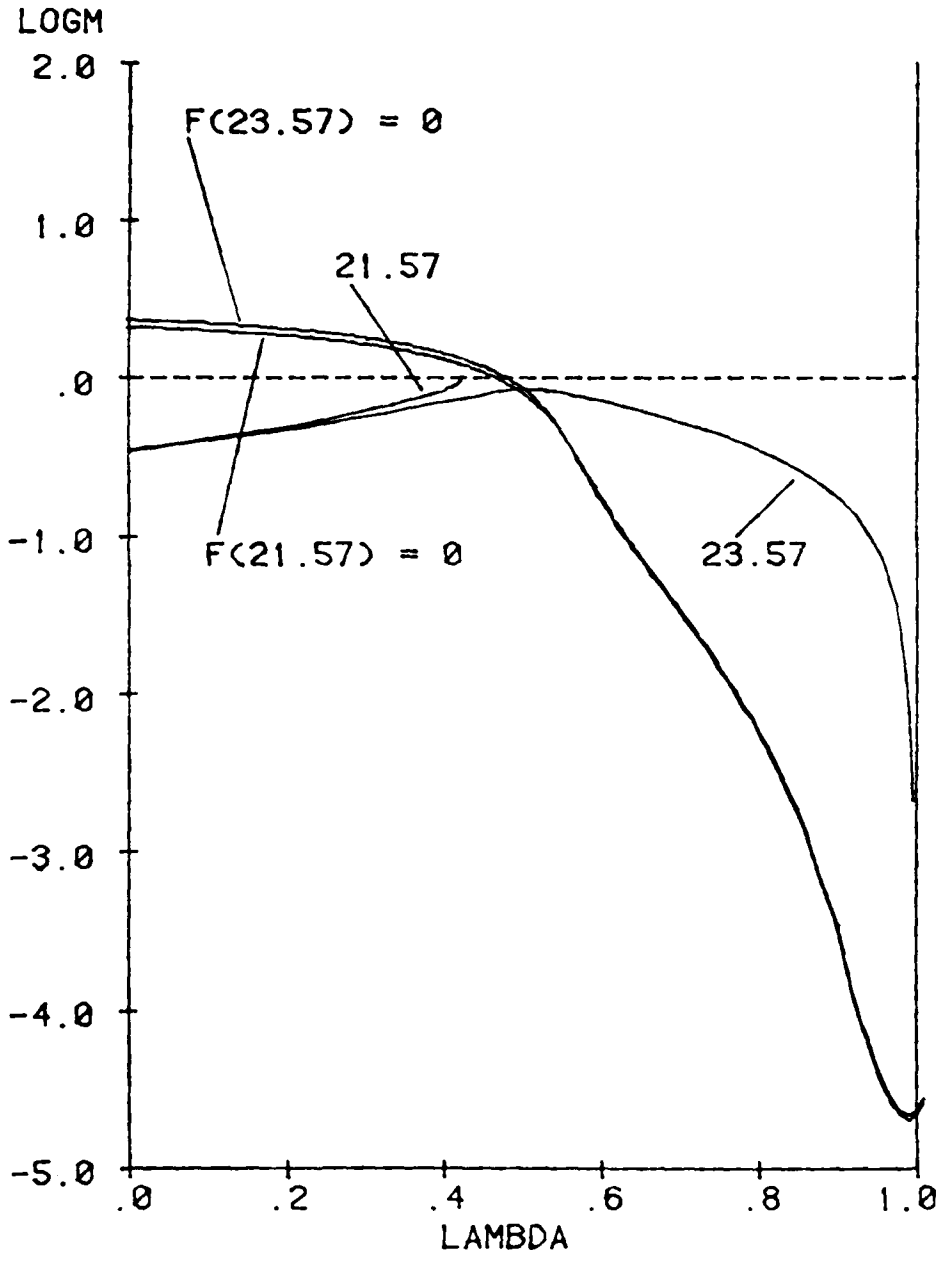

G=V= 3.000

B	RV	M0	EPSILO	TYPE
6.830	.102	21.570	.0600000	2
6.830	.102	23.570	.0600000	1

FIGURE 2

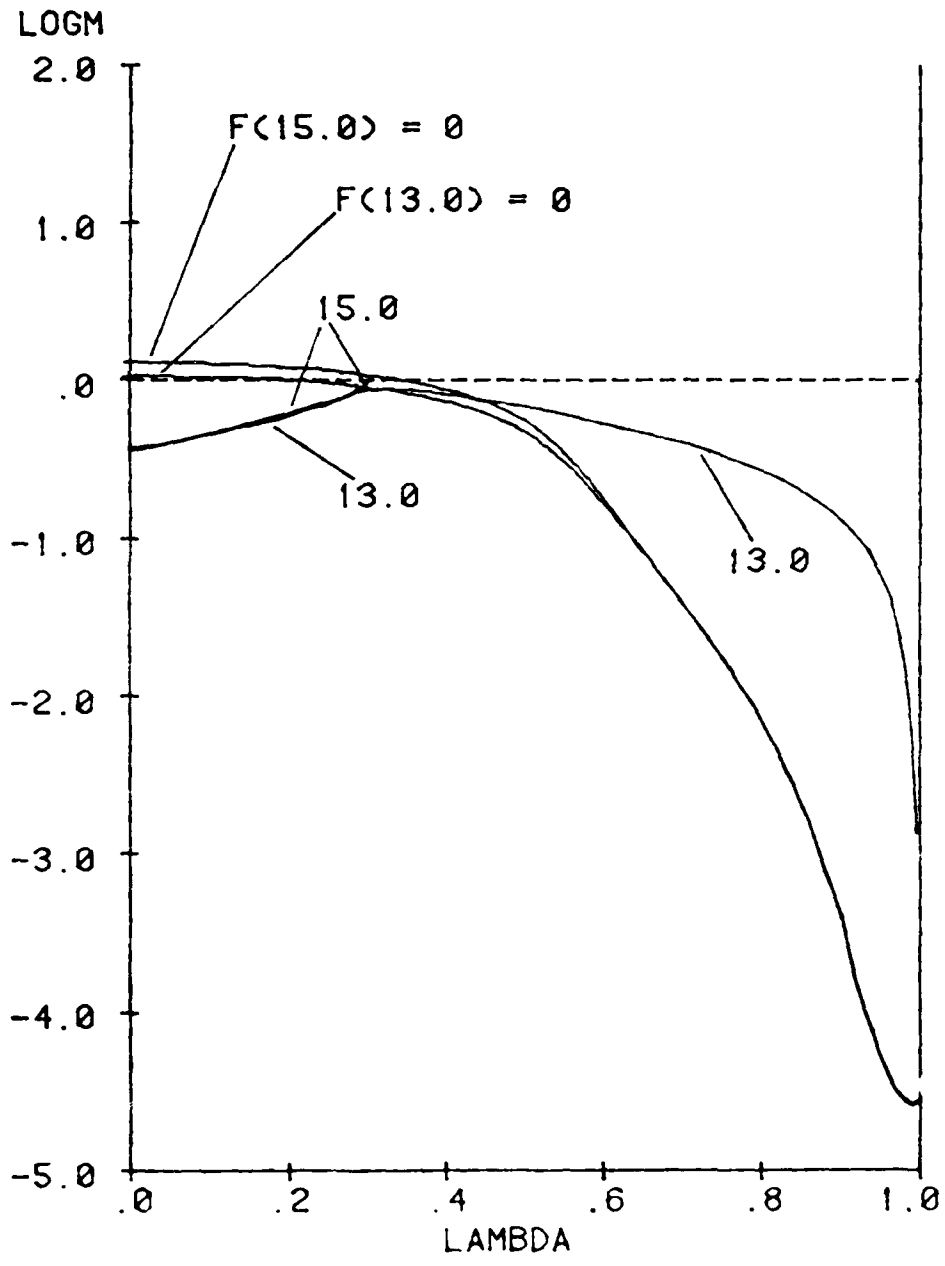

G=V= 3.000

B	RV	M0	EPSILO	TYPE
6.830	.102	13.000	.0600000	1
6.830	.102	15.000	.0600000	2

FIGURE 3

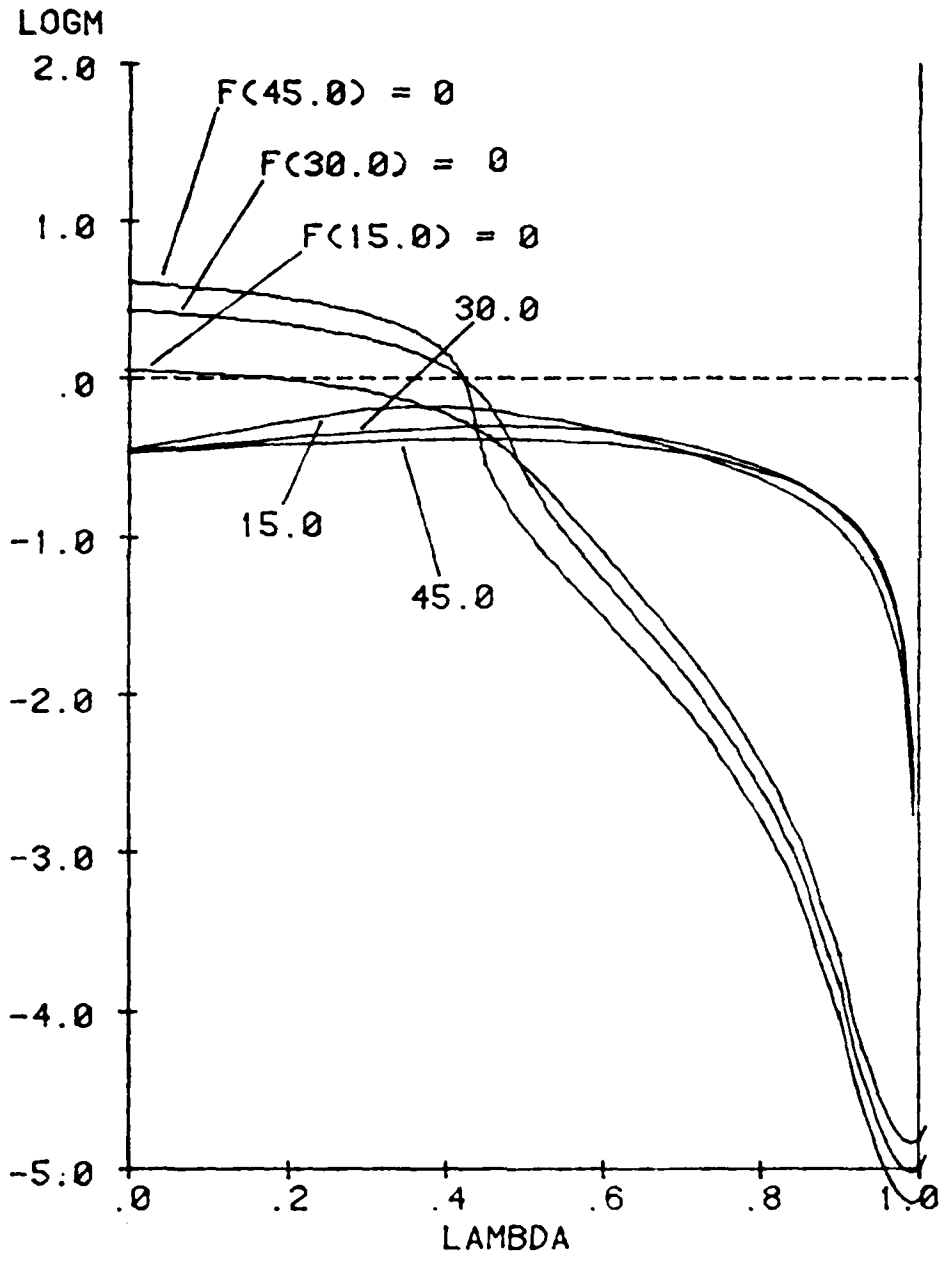

G=V= 3.000

B	RV	M0	EPSILO	TYPE
6.830	.102	15.000	.0800000	1
6.830	.102	30.000	.0800000	1
6.830	.102	45.000	.0800000	1

FIGURE 4

BEHAVIOR OF TRAJECTORIES IN S & W REGIONS

M01 < M02 < M03

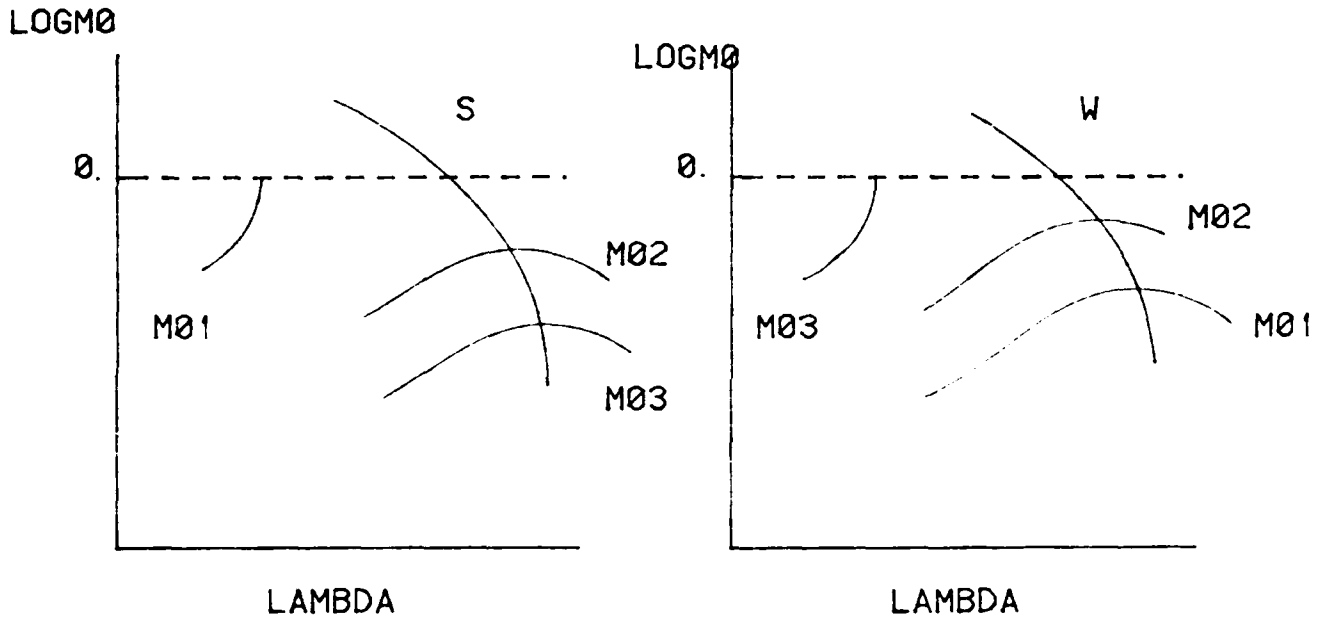

FIGURE 5

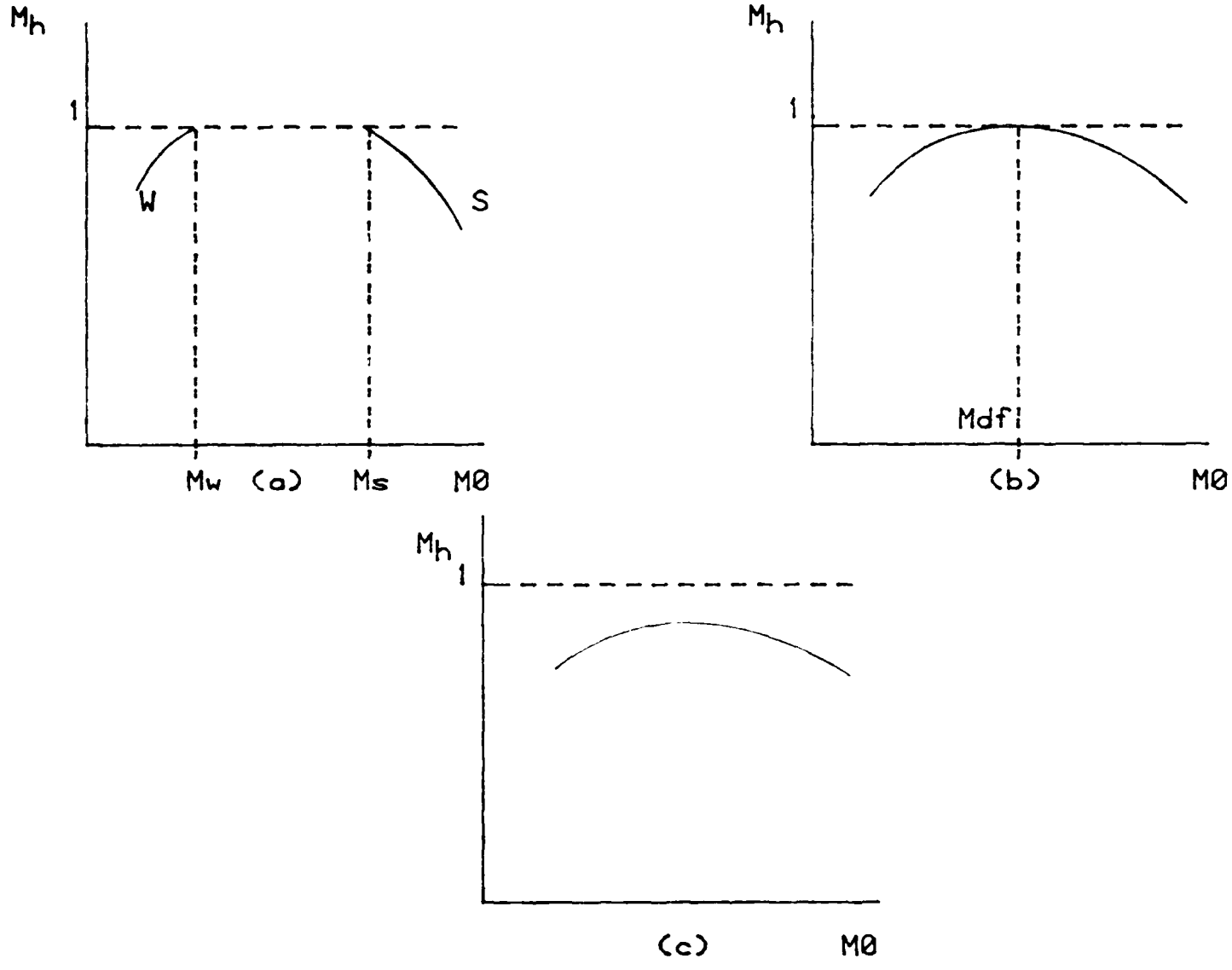

FIGURE 6

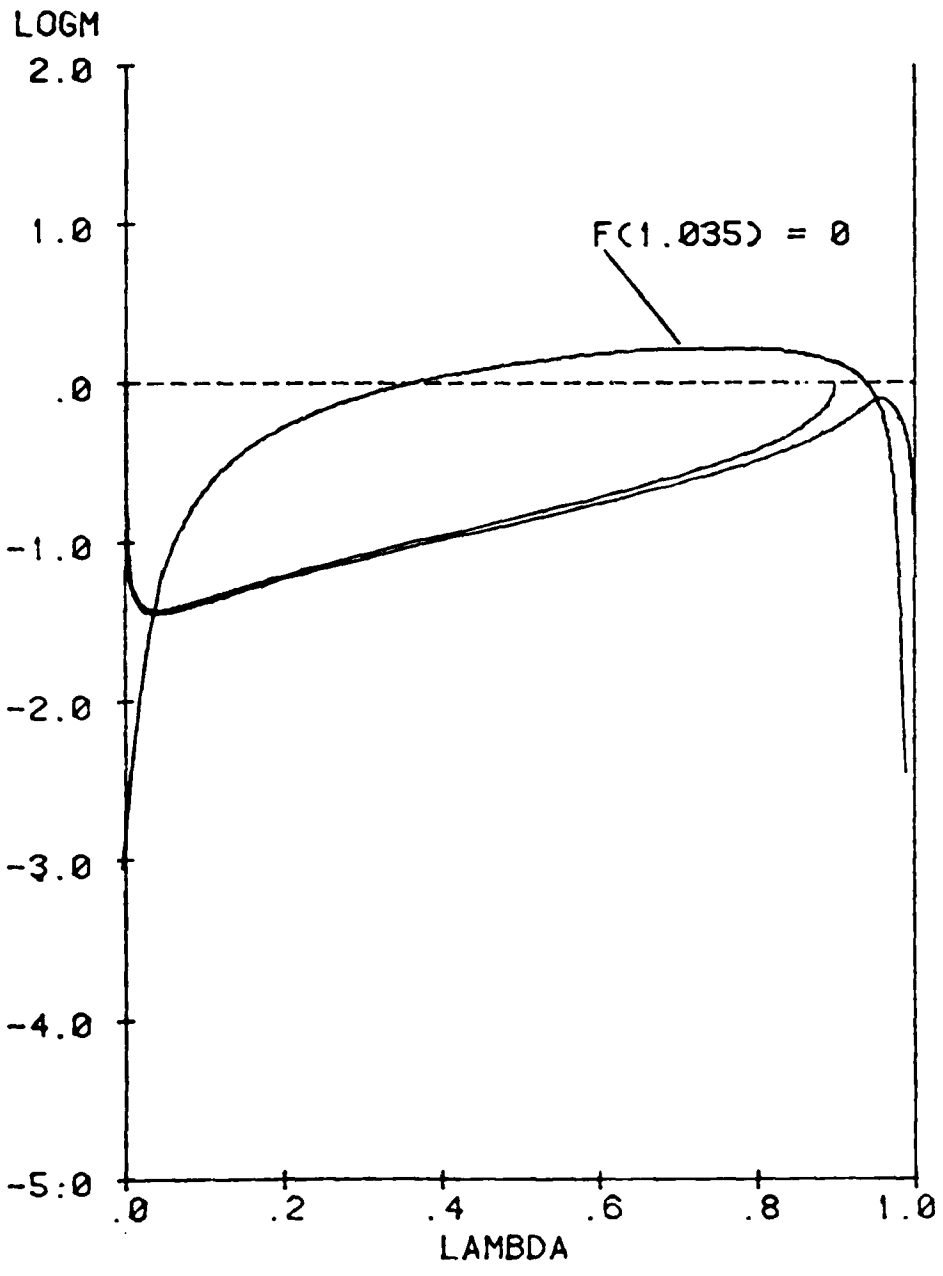

G=V= 3.000

B	RV	M0	EPSILO	TYPE
6.830	.102	1.030	.0001000	1
6.830	.102	1.040	.0001000	2

FIGURE 7

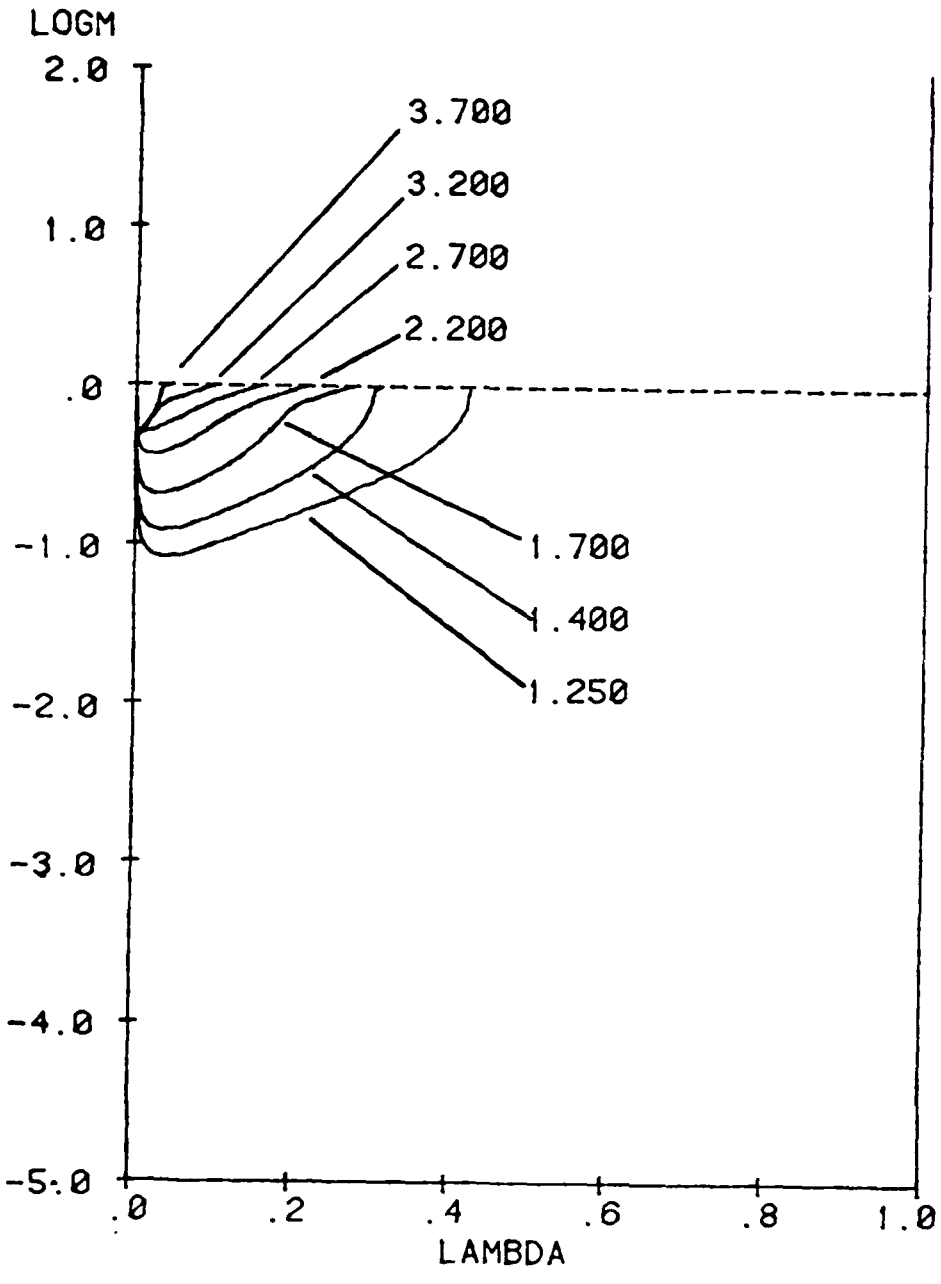

G=V= 3.000

B	RV	M0	EPSILO	TYPE
6.830	.102	1.250	.0001000	2
6.830	.102	1.400	.0001000	2
6.830	.102	1.700	.0001000	3
6.830	.102	2.200	.0001000	3
6.830	.102	2.700	.0001000	3
6.830	.102	3.200	.0001000	3
6.830	.102	3.700	.0001000	2

FIGURE 8

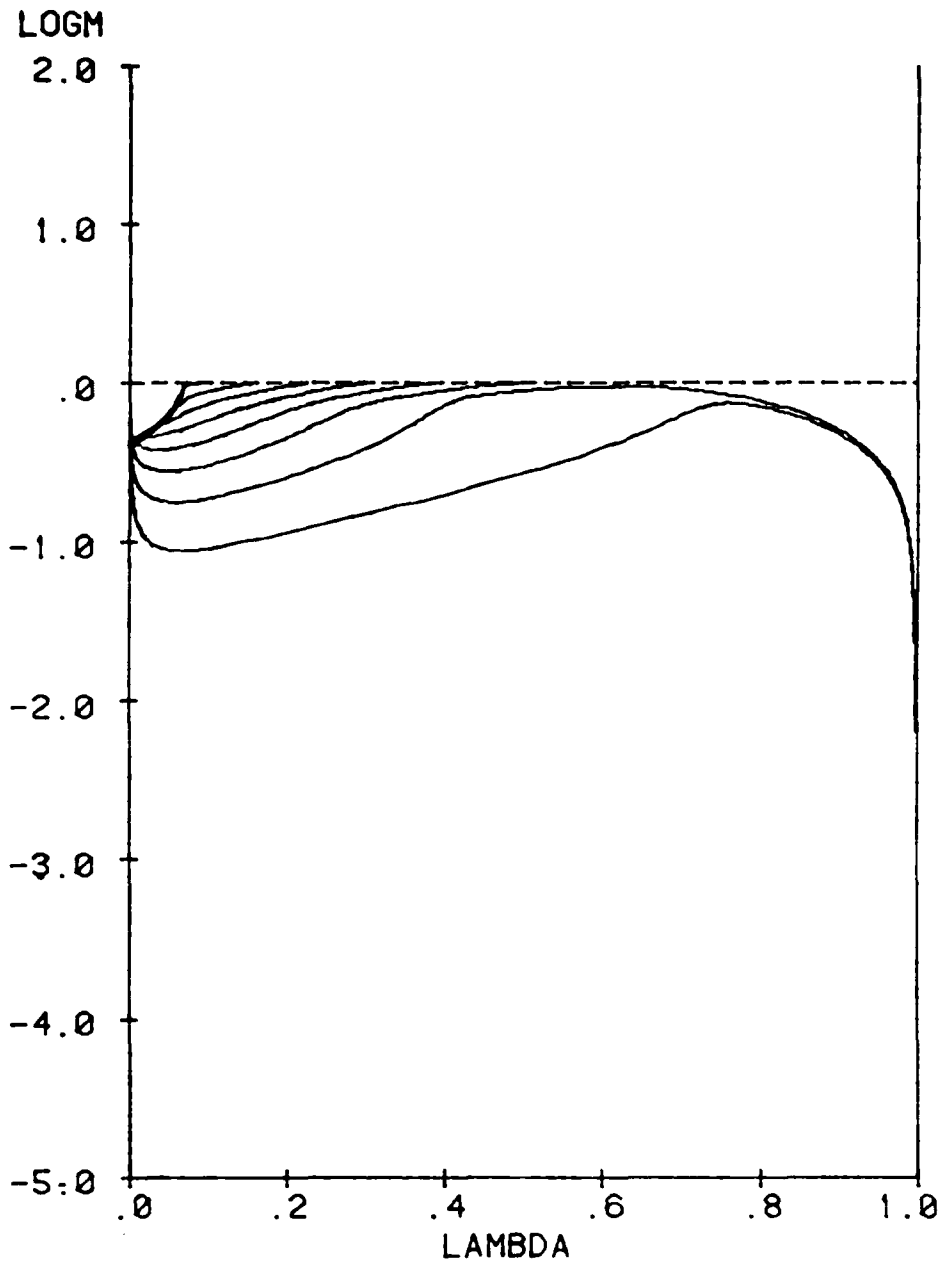

G=V= 3.000

B	RV	M0	EPSILO	TYPE
6.830	.102	2.000	.0025000	1
6.830	.102	2.500	.0025000	1
6.830	.102	3.000	.0025000	3
6.830	.102	3.500	.0025000	3
6.830	.102	4.000	.0025000	3
6.830	.102	4.500	.0025000	3
6.830	.102	5.000	.0025000	3
6.830	.102	5.500	.0025000	3
6.830	.102	6.000	.0025000	2
6.830	.102	6.500	.0025000	2

FIGURE 9

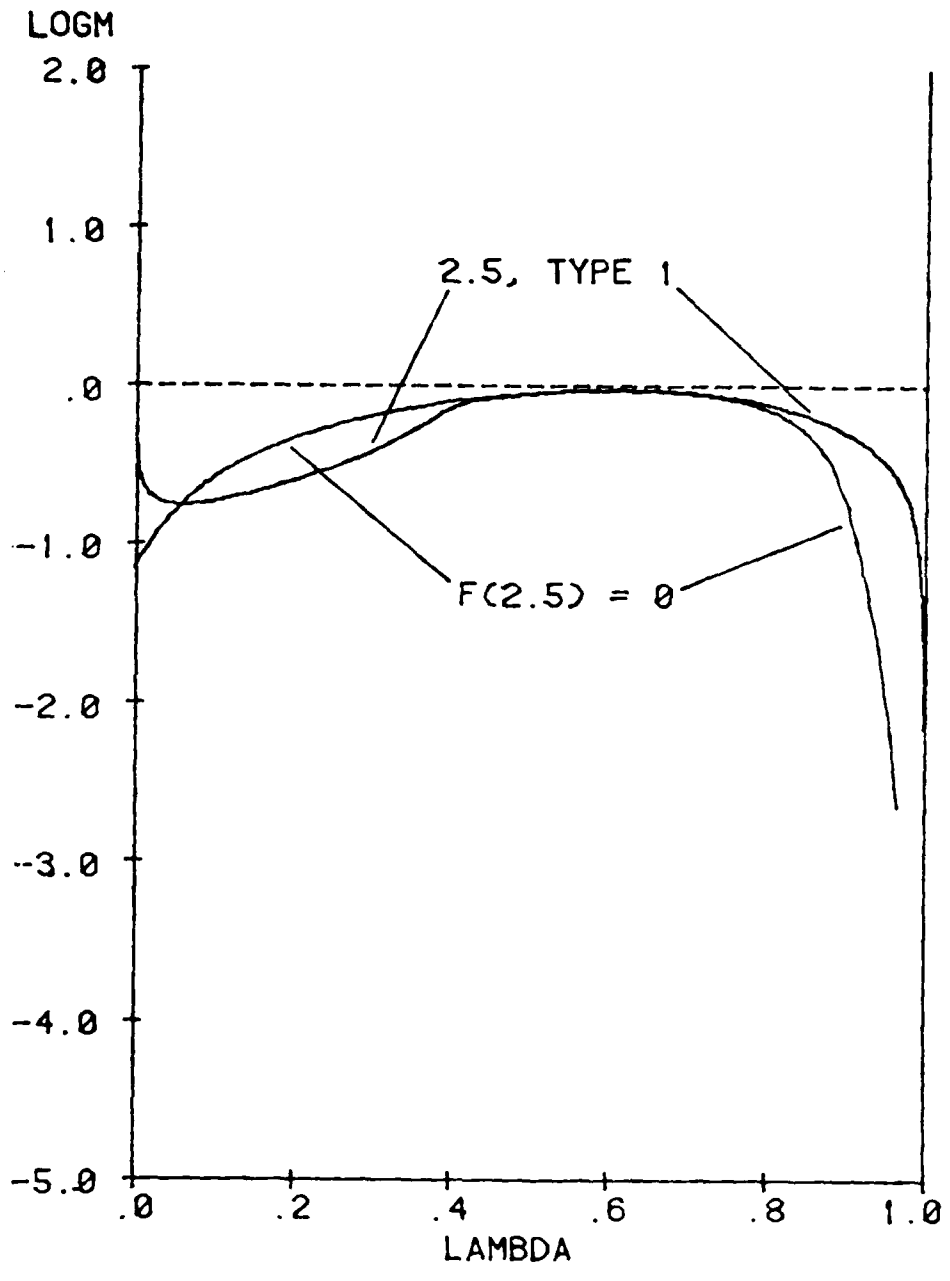

G=V= 3.000

B	RV	M0	EPSILO
6.830	.102	2.500	.0025000

FIGURE 10

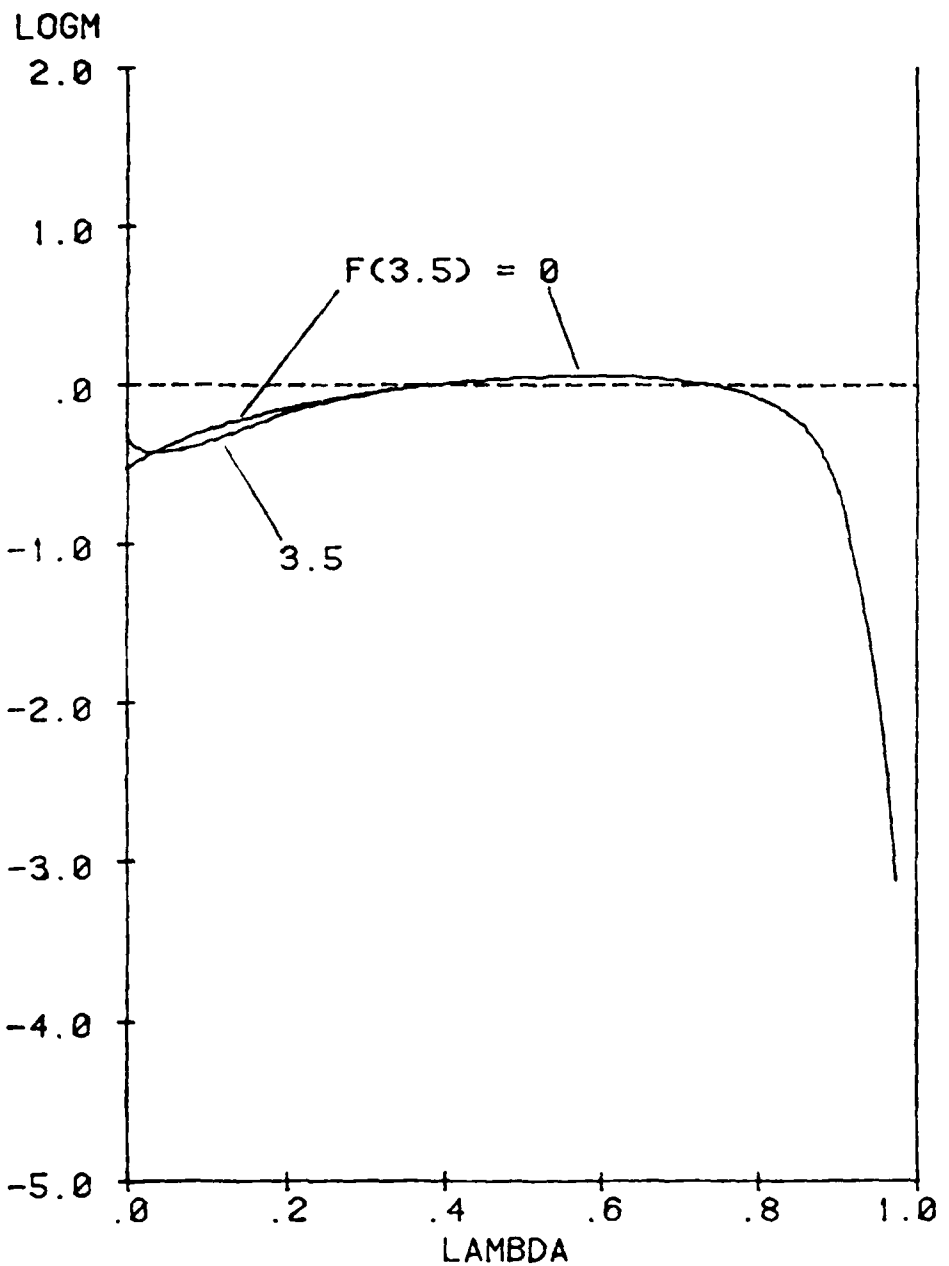

G=V= 3.000

B	RV	M0	EPSILO	TYPE
6.830	.102	3.500	.0025000	3

FIGURE 11

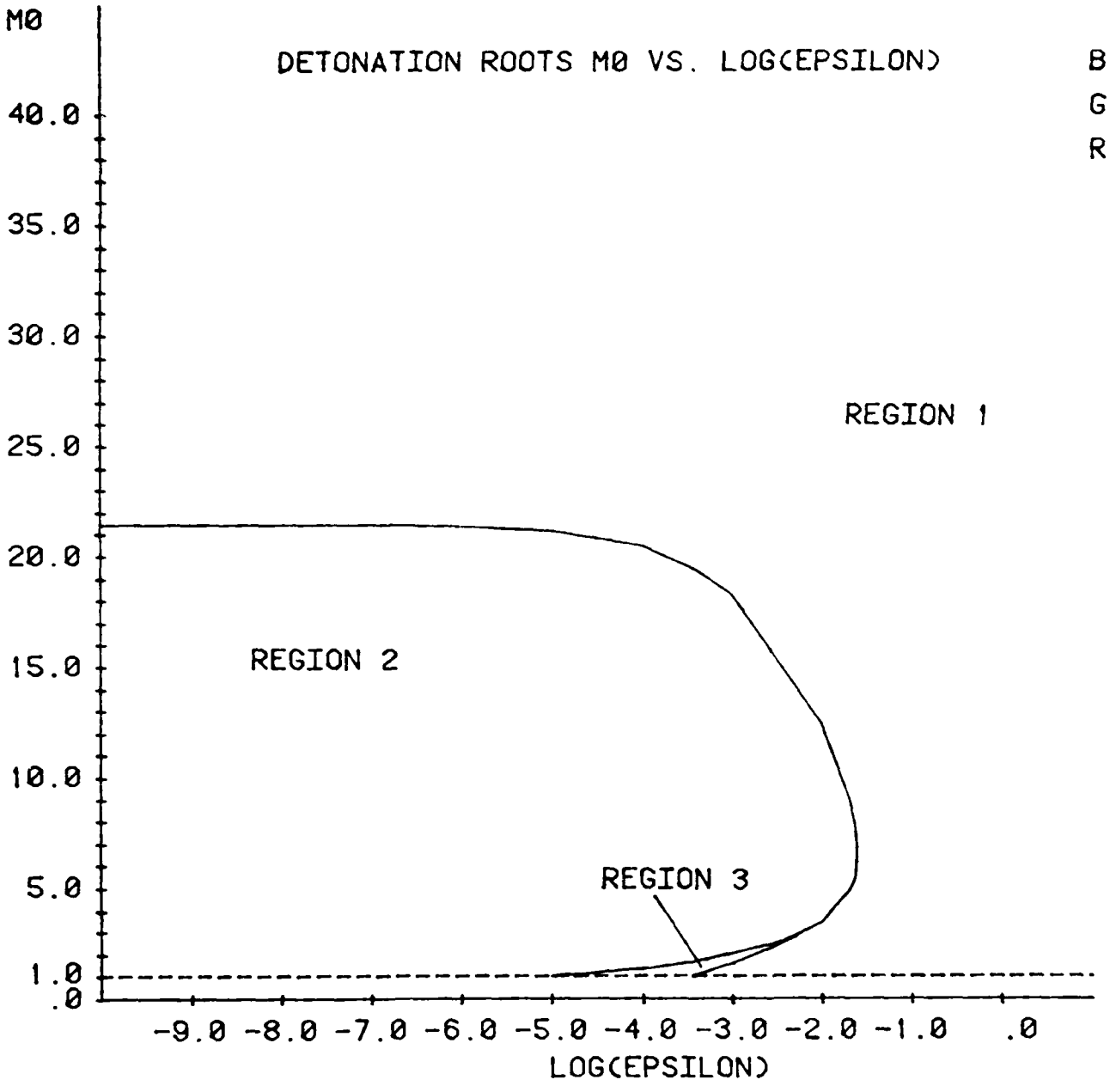
M0
DETONATION ROOTS M0 VS. LOG(EPSILON)
B = 12.500
G = 3.000
R = .410
40.0
35.0
30.0
25.0
20.0
15.0
10.0
5.0
1.0
.0
REGION 1
REGION 2
REGION 3
-9.0 -8.0 -7.0 -6.0 -5.0 -4.0 -3.0 -2.0 -1.0 .0
LOG(EPSILON)

FIGURE 12

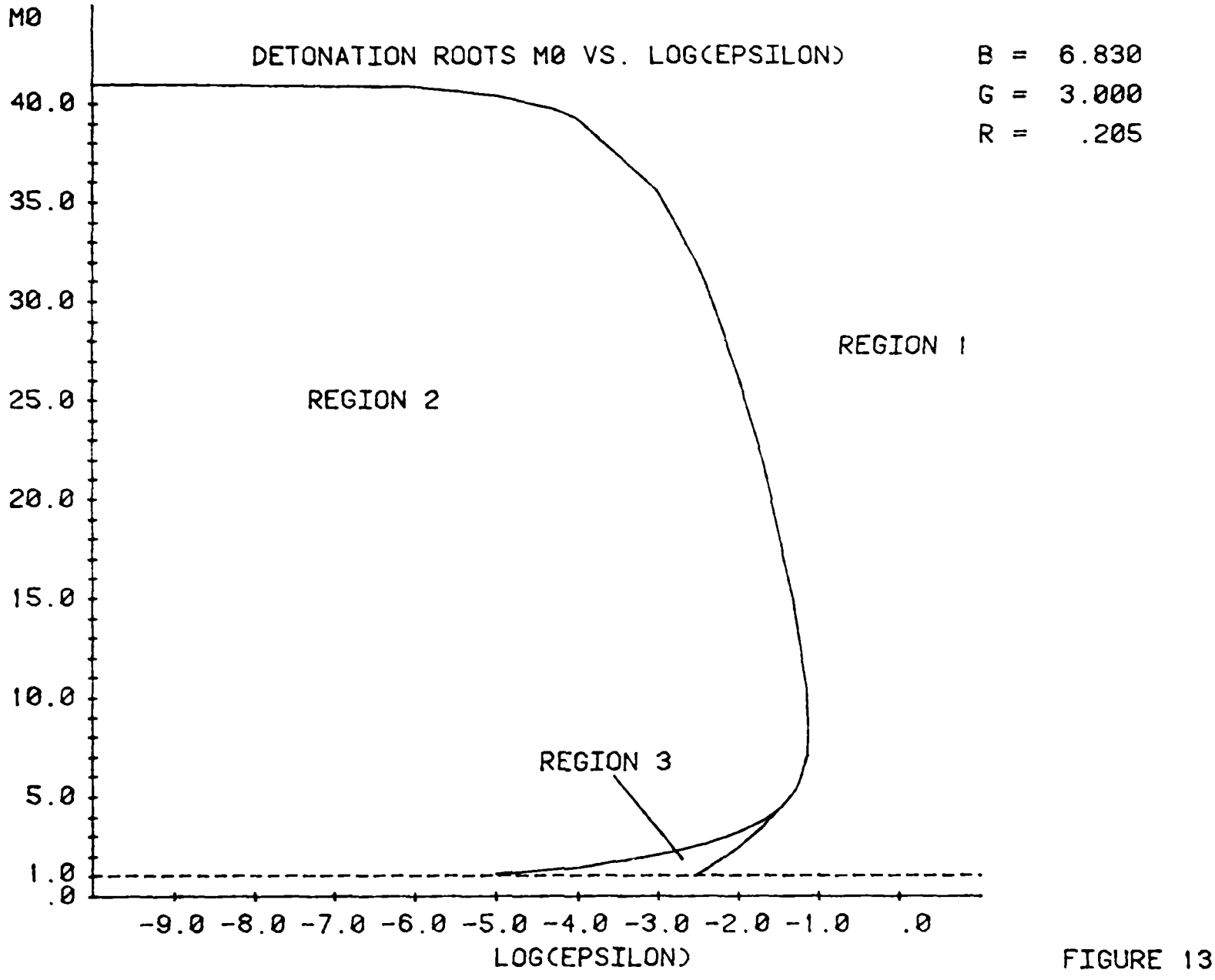
M0
DETONATION ROOTS M0 VS. LOG(EPSILON)
B = 6.830
G = 3.000
R = .205
40.0
35.0
30.0
25.0
20.0
15.0
10.0
5.0
1.0
.0
REGION 1
REGION 2
REGION 3
-9.0 -8.0 -7.0 -6.0 -5.0 -4.0 -3.0 -2.0 -1.0 .0
LOG(EPSILON)

FIGURE 13

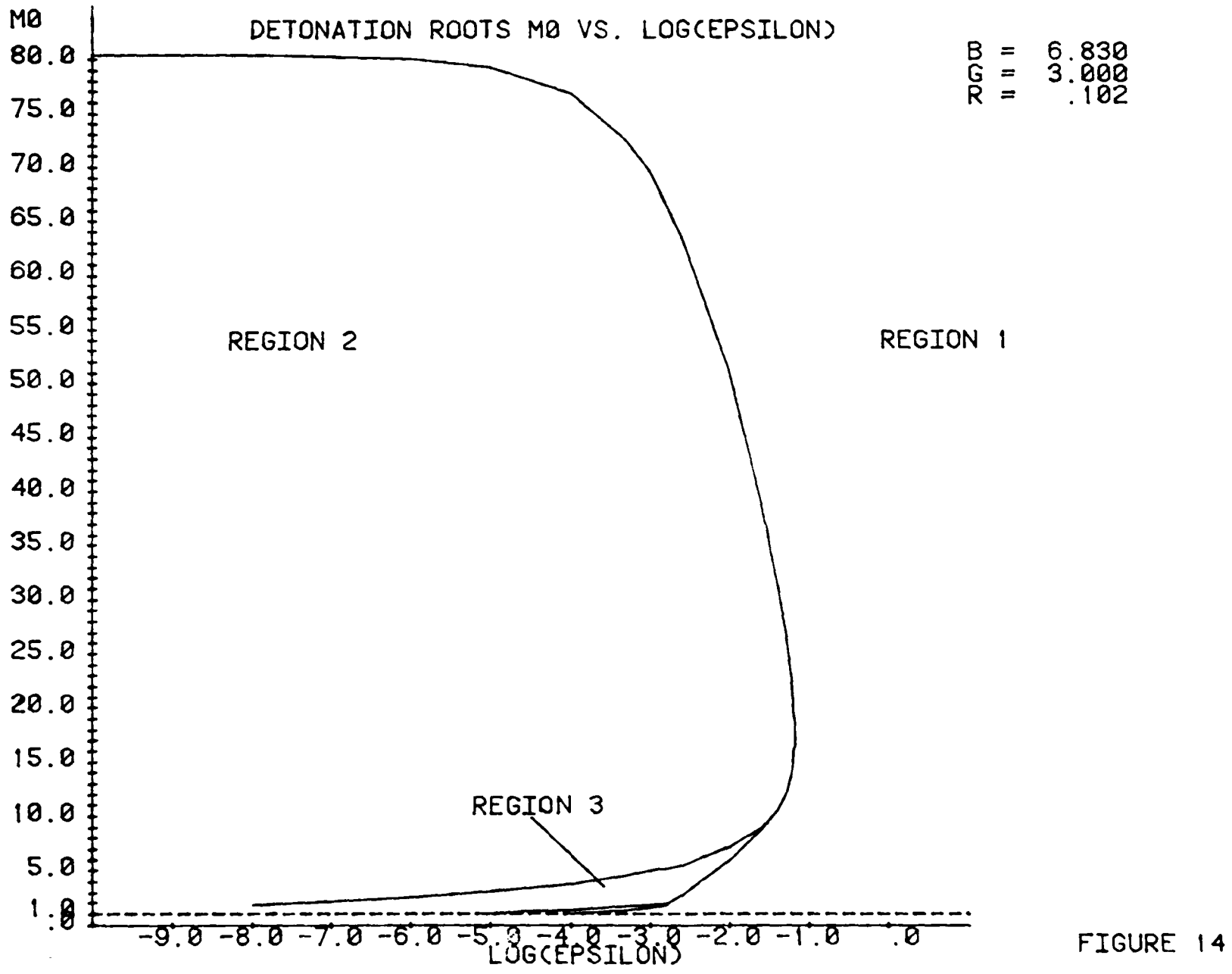
M0
DETONATION ROOTS M0 VS. LOG(EPSILON)
B = 6.830
G = 3.000
R = .102
80.0
75.0
70.0
65.0
60.0
55.0
50.0
45.0
40.0
35.0
30.0
25.0
20.0
15.0
10.0
5.0
1.0
.0
REGION 2
REGION 1
REGION 3
-9.0 -8.0 -7.0 -6.0 -5.0 -4.0 -3.0 -2.0 -1.0 .0
LOG(EPSILON)

FIGURE 14

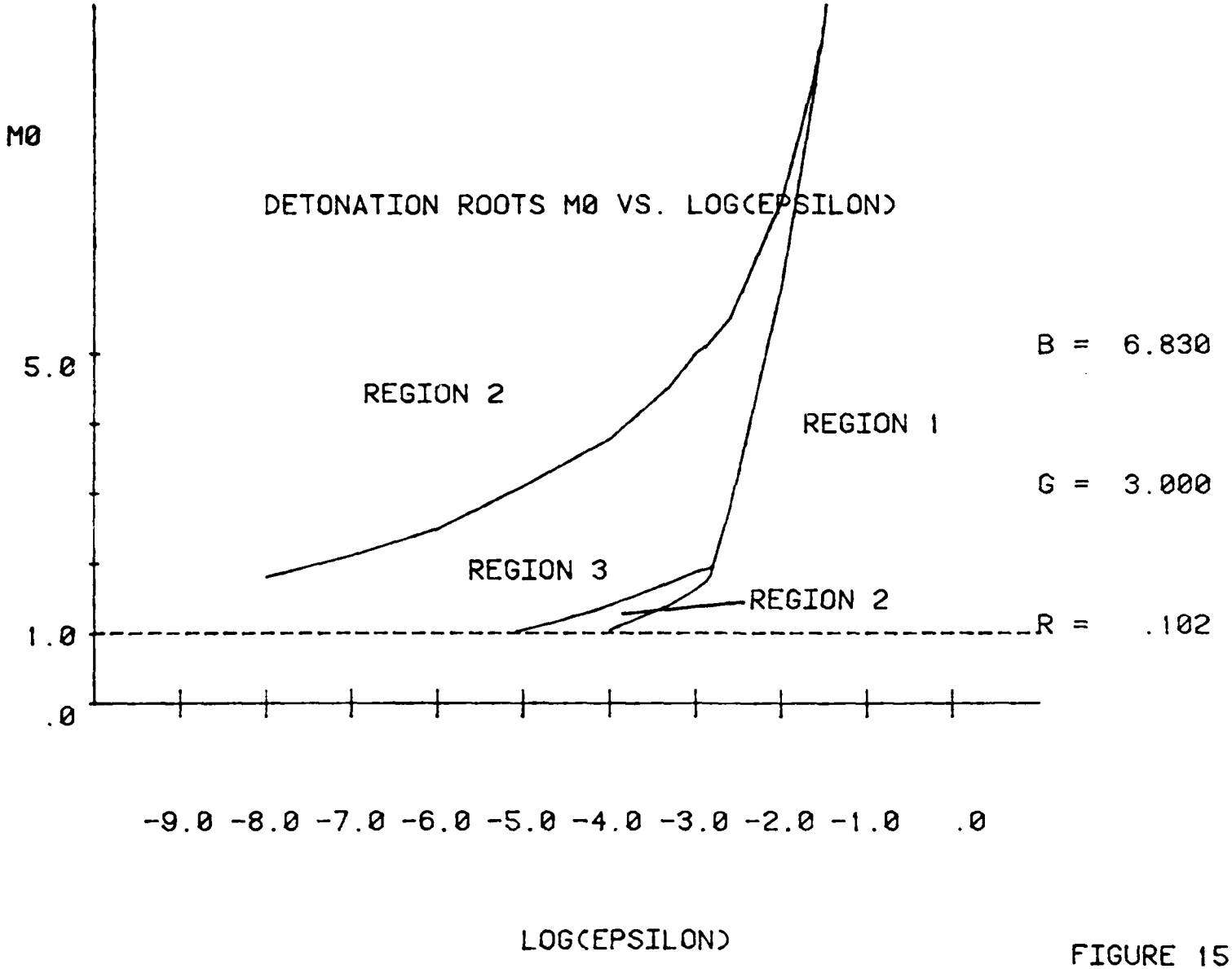
M0
DETONATION ROOTS M0 VS. LOG(EPSILON)
5.0
1.0
.0
REGION 2
REGION 1
REGION 3
REGION 2
B = 6.830
G = 3.000
R = .102
-9.0 -8.0 -7.0 -6.0 -5.0 -4.0 -3.0 -2.0 -1.0 .0
LOG(EPSILON)

FIGURE 15

PROPOSAL TO AIR FORCE OFFICE OF SCIENTIFIC RESEARCH

Attention: Dr. Michael A. Stroscio
AFOSR/NP
Bolling AFB
D.C. 20332

Proposing Institution : University of Miami
Department of Physics
Coral Gables, FL 33124

Title : Numerical and Analytical Studies of Steady Detonation Waves with Expansion Losses.

Budget : $ 29,186

Proposed Duration : July 1, 1982 - June 30, 1983.

Principal Investigator : Dr. Manuel A. Huerta
Associate Professor of Physics
University of Miami
[redacted]

Manuel A. Huerta
Signature of P.I.

Date : 2/19/'82

Manuel A. Huerta
Chairman, Department of Physics

Date : 2/19/'82

Ronald E. Siegwald
Authorized Official
Ronald E. Siegwald
Director, Sponsored Programs/Fiscal Management.

Date : 2/22/82

TABLE OF CONTENTS

Description of Proposed Research.....pages 3-9

References.....page 10

Figures.....pages 11-12

Plan of Work and Budget Justification.....page 13

Budget.....pages 14-15

P.I.'s Curriculum Vita.....pages 16-21

ABSTRACT

Numerical integration of the steady detonation and deflagration equations with a model expansion loss and reaction rate can give four propagation speeds. The first two are a fast (strong) and a slow (weak) detonation solutions . The other two are a fast (weak) and a slow (strong) deflagration solutions. The two weak solutions join at Mach one at a value of the loss that depends on the other parameters of the problem. These calculations should be expanded to different dependences on the reaction progress variable. Approximate analytical results that confirm the above numerical calculations have been obtained. These results need to be pursued because they could help to understand the influence of loss terms on detonation waves.

DESCRIPTION OF PROPOSED RESEARCH

INTRODUCTION

I propose to study the existence of multiple propagation speeds and detonation failure for steady detonation waves in the presence of expansion losses. The treatment is based entirely on the model developed in Sec.5G of the book by Fickett and Davis[1]. As discussed in Ref.1, we do not consider the complete two dimensional flow in a cylindrical explosive charge. This would entail the solution of a free boundary value problem of great complexity. Rather the equations are specialized to the x-axis where the radial velocity ω vanishes by symmetry. The divergence $\partial\omega/\partial x$ is put in as a function of x obtained from some approximation. Much can be learned from the study of the remaining equations into which $\partial\omega/\partial x$ is inserted. Their phase plane is sufficiently complicated that unexpected behavior is possible.

We introduce an expansion loss parameter defined by

$$\epsilon = \frac{1}{A}\frac{dA}{dx} = \frac{2}{u}\frac{\partial\omega}{\partial r}$$

where u is the x-component of fluid velocity. The equations take the form of nozzle flow with variable cross-sectional area A in the quasi-one-dimensional approximation. The equations are valid in the region from $x = 0$, where the reaction zone begins, to the end of the reaction zone that occurs at the sonic point $u = c$. As in Ref.1, the unsteady region connecting the sonic point to the rear boundary condition is not considered here. With the above restrictions, the equations are

$$\frac{d(\rho u A)}{dx} = 0 \quad ,$$

$$\frac{du}{dx} = \frac{(\sigma R - u\varepsilon)}{(1 - u^2/c^2)} \quad ,$$

$$\frac{d\lambda}{dx} = \frac{R}{u} \quad ,$$

and

$$d(H + u^2/2)/dx = 0 \quad ,$$

where

$$H = \frac{\gamma p}{(\gamma-1)\rho} - \lambda q = \frac{c^2}{(\gamma-1)} - \lambda q \quad ,$$

with all the quantities defined as usual in Ref. 1. These equations can be put into a form where the only variables are the Mach number squared, $m = u^2/c^2$, and the reaction progress variable, λ. These equations are

$$\frac{2(1-m)dm/dx}{m(1+\gamma m)(2+(\gamma-1)m)} = \frac{d(\sum\lambda_i q_i)/dx}{\sum\lambda_i q_i + h_1 + u_1^2/2} - \frac{2\varepsilon}{1+\gamma m} \quad , \qquad (1)$$

$$\frac{d\lambda_i}{dx} = \frac{R_i}{u} \quad , \qquad (2)$$

and

$$c^2 = \frac{2(\gamma-1)}{2 + (\gamma-1)m} \left(\sum\lambda_i q_i + h_1 + u_1^2/2\right) \quad .$$

We are in the frame of the reaction front. The unreacted explosive fluid approaches from $x < 0$ with a velocity D to be determined. D will be obtained

in terms of the Mach number squared $m_0 = D^2/c_0^2$ at $x = 0^-$. We can discuss both the detonation and deflagration solutions with Eqs.(1) and (2). For the detonation case there is a shock at $x = 0$. The Mach number squared $m_1 = (u_1/c_1)^2$ at $x = 0^+$ is related to m_0 by the usual Hugoniot relations[2]

$$m_1 = \frac{2 + (\gamma-1)m_0}{2\gamma m_0 - (\gamma-1)} ,$$

and

$$c_1^2 = c_0^2 \frac{(2\gamma m_0-(\gamma-1))(2+(\gamma-1)m_0)}{m_0(\gamma+1)^2} .$$

For the deflagration solutions there is no shock at $x = 0$, so $m_0 = m_1$, and $c_0 = c_1$.

Several authors have considered this model with different reaction rates R_i and expanson terms ε. Wecken[3] considered the case ε = constant and obtained partial results on multiple solutions and detonation failure. Tsuge[4] et al., and Fujiwara and Tsuge[5] have integrated the nozzle equations numerically for a hydrogen/oxygen detonation with a good model for the lateral expansion. They have shown that sufficiently great expansion losses lead to detonation failure. They also obtain two detonation speeds that join at the failure diameter. For small losses the fast root goes to the Chapman-Jouguet value. They conjectured that the slow root went to Mach one as the losses decreased to zero (charge diameter$\longrightarrow\infty$). They were not able to verify it due to the large amounts of computer time required.

PREVIOUS WORK BY THE PRINCIPAL INVESTIGATOR

I have obtained preliminary results that show the existence of 2 detonation roots and 2 deflagration roots together with detonation and deflagration failure. Specifically, Eqs.(1) and (2) have been integrated numerically with ε = constant and a model reaction rate

$$R = (c/L)\ (T_a/T + 1)\ \exp(-T_a/T)\ (1 - \lambda)^2 \quad , \qquad (3)$$

where L is a reaction length and T_a is an activation temperature. This form for R was chosen partly to compare the numerical results with the analytical approximation discussed below. Using $T = M_w c^2/R_o\gamma$, where M_w is molecular weight, and R_o is the gas constant, we write

$$\frac{T_a}{T} = B\,\frac{2 + (\gamma-1)m}{(\gamma+1)(\lambda+h)} \quad ,$$

where

$$h = (H_1+u_1^2/2)/q = c_0^2\,\frac{(2+(\gamma-1)m_0)}{q(\gamma-1)} \quad ,$$

and

$$B = \gamma R_o T_a(\gamma+1)/(2qM_w(\gamma-1)) \quad .$$

The phase plane of Eqs.(1) and (2) can look very different depending on the values of the parameters and on the value of m_0. A typical case is shown in Fig.1. Let Ω be the right hand side of Eq.(1). The curves $\Omega = 0$ and $m = 1$ are shown in Fig.1. For a given value of m_0 the phase orbit starts at $\lambda = 0$, $m = m_1$ and crosses the line $\Omega = 0$; this is an orbit of type 1. For another value of m_0 the phase orbit reaches the line $m = 1$ with a vertical slope ; this is an orbit of type 2. The above values of m_0 bracket the correct value. The correct solution is the one where dm/dx remains finite at $m = 1$ so that it can be joined to the rear flow behind the sonic point. The correct orbit shown in Fig. 1 passes through the critical point at $m = 1$, $\Omega = 0$. The

problem is not an initial value problem but rather a boundary value problem that yields the value for m_0. Its form is suitable for a Nonlinear Shooting Method[6]. We start with a very low value for m_0, say 0.01, get that orbit, and increase m_0. When the type of the orbit changes we have bracketed the desired value of m_0. This procedure is done for each value of ε.

With fairly realistic values for the parameters $c_0^2/q = 0.41$, $\gamma = 3$, and $B = 12.5$, the results obtained for m_0 as a function of ε are shown in Fig. 2 where $\log m_0$ is plotted versus $\log\varepsilon$. The curve separates the regions of type 1 and type 2 in the $\log m_0$-$\log\varepsilon$ plane. Branch A is the fast (strong) detonation branch. It joins the slow (weak) detonation branch at $\varepsilon_1 \approx 0.0246$. For $\varepsilon > \varepsilon_1$, there are no steady solutions. This is the value for detonation failure. The slow detonation branch ends at Mach one at the value $\varepsilon_3 \approx 10^{-5}$ (the possible singularity at $m_0 = 1$ is not as dangerous as it might appear). There it joins the fast (weak) deflagration branch C. Branch C joins the slow (strong) deflagration branch D at $\varepsilon_2 \approx 2.1\text{x}10^{-5}$. This is the deflagration failure value. The bend in the fast deflagration branch occurs at $\varepsilon_4 \approx 0.97\text{x}10^{-7}$. It is clear that the slow detonation branch does not go to Mach one at $\varepsilon = 0$, but at $\varepsilon = \varepsilon_3$. In Fig. 2 one can see that for $\varepsilon < \varepsilon_4$ there are the two normal roots, a deflagration and a detonation root. For $\varepsilon_4 < \varepsilon < \varepsilon_2$ there are four roots, while for $\varepsilon_2 < \varepsilon < \varepsilon_1$ there are the two detonation roots.

The reaction zone thickness varies widely as m_0 and ε are varied. It ranges from the order of 20L to the order of 100,00L. For this reason some calculations take much more CPU time than others. This is because the computer program integrates as far as needed until it reaches either $\Omega < 0$ (type 1) or

$m > 1$ (type 2). A full run of m_0 values for a particular value of ε may take 15 minutes of CPU time without using double precision. The CPU time is as small as this thanks to the use of a Runge-Kutta-Fehlberg[7] method with its variable step size and error control to integrate the differential equations. Fortunately when the reaction thickness is very large the solutions vary slowly so the method can take large step sizes, say 50L. For the small reaction zones, however, the step sizes are much smaller.

PROPOSED WORK

I propose to continue the numerical calculations just described. It is necessary to use double precision in at least some ranges to be fairly sure of the results. Also one should use a variety of parameter values and reaction rates R. This would show how a different λ dependence in R affects the results.

I would also like to pursue obtaining qualitative results that help to understand the numerical ones. For example, I have done a problem with

$$\frac{d\lambda}{dx} = \frac{R_s}{u_s} (1-\lambda)^2 \quad ,$$

where R_s is the value (constant in x) of the R given in Eq.(3) at the sonic point, and u_s is the value (also constant in x) of u at the sonic point. With a further approximation for the x dependence of ε, I have been able to integrate Eqs.(1) and (2) exactly. The results are two nonlinear algebraic equations whose simultaneous solution yields m_0. The results give a curve very much like that of Fig. 2. Furthermore the algebraic equations obtained give a good graphical reason for why there should be 4 roots.

REFERENCES

1. Fickett, W. and Davis, W.C., Detonation. Berkeley : University of California Press. 1979.

2. Landau, L.D., and Lifshitz, E.M., Fluid Mechanics, Addison-Wesley, Mass. 1959.

3. Wecken, F., 'Non-Ideal Detonation with Constant Lateral Expansion'. In Fourth Symposium (International) on Detonation, pp.107-116. Washington, D.C. Office of Naval Research - Department of the Navy (Acr-126) (1965).

4. Tsuge, S., et al.,Astronaut. Acta 15, 377 (1970).

5. Fujiwara, T., and Tsuge, S., J. Phys. Soc. Japan 33, 237 (1972).

6. Burden, R.1., et al., Numerical Analysis, Prindle, Weber and Scmidt, Boston, Mass. (1978). Section 10.2

7. ibid, Section 6.5.

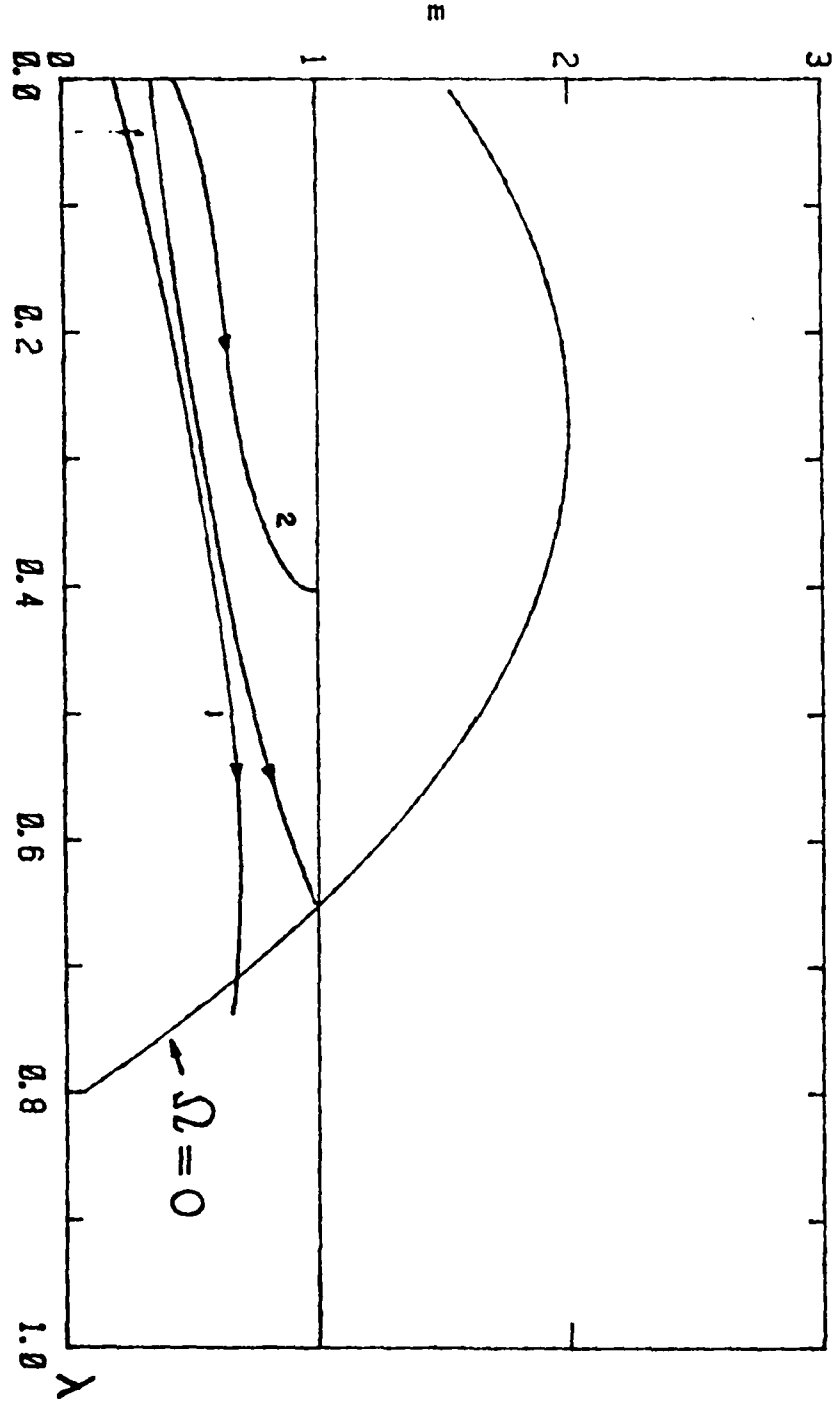

FIGURE 1

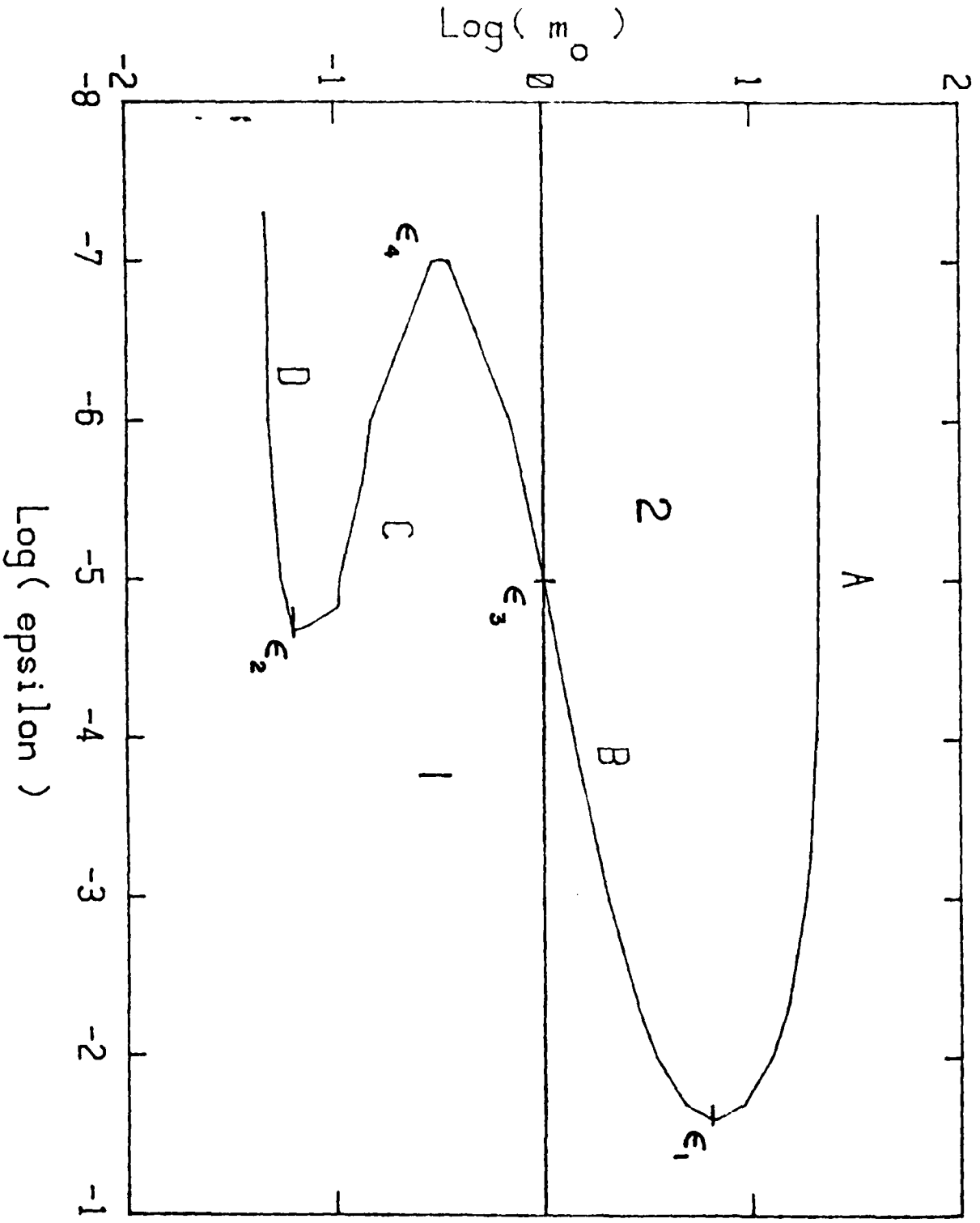
Log(m_o)
-2
-1
0
1
2
-8
-7
-6
-5
-4
-3
-2
-1
Log(epsilon)
ε_4
ε_2
ε_3
ε_{-1}
A
B
C
D
1
2

FIGURE 2

PLAN OF WORK AND BUDGET JUSTIFICATION

I plan to work full time on the above problems from July 1 to August 15, 1982, and from May 15 to June 30, 1983. This constitutes 3 months of summer work during the one year period of this proposal. The University of Miami has a fast Univac 1100/81 main frame computer and many terminals on campus. During the day, runs that request sizable amounts of CPU time are given a low priority so the turn around time can be quite slow. The runs could be submitted in batch mode but that destroys the advantages of demand mode where one can submit a run, inspect the results, vary the step size, and so on. I believe these conditions justify my request for a computer terminal and a modem to install in my home. This way I can submit runs at night when the load on the Univac is much less and the turn around time is very short.

STATEMENT OF OTHER SUPPORT

The previous work by the P.I. on detonation problems was done mostly under AFOSR minigrant No.AFOSR80-0135. That minigrant expired in the summer of 1981. The P.I. does not have any other research support at this time.

BUDGET

July 1, 1982 - June 30, 1983

1. SALARIES AND WAGES		
Principal Investigator - Dr. M. Huerta		
Full time 1½ months summer, 1982	5,525.	
Full time 1½ months summer, 1983	5,967.	
	11,492.	
Fringe Benefits @ 19.35%	2,224.	
TOTAL SALARIES AND WAGES		13,716.
2. PERMANENT EQUIPMENT		
Hazeltine Esprit Computer Terminal with Koch modifications	800.	
1200 baud telephone modem	600.	
TOTAL EQUIPMENT		1,400.
3. EXPENDABLE SUPPLIES AND MATERIALS		200.
4. TRAVEL (DOMESTIC)		
One scientific meeting and one visit to another institution:		
Estimated r.t. air fare @ $350/trip 2 x $350	700.	
3 days per diem/trip @ $75/day 2 x 3 x $75	450.	
Local transportation @ $25/trip 2 x $25	50.	
TOTAL TRAVEL		1,200.
5. PUBLICATION COSTS		700.

BUDGET

July 1, 1982 - June 30, 1983

(continued)

6.	OTHER COSTS		
	Computer Time	1,500.	
	Long Distance Telephone	50.	
	TOTAL OTHER COSTS		1,550.
7.	TOTAL DIRECT COSTS		18,766.
8.	INDIRECT COSTS (see note below)		
	60% Modified Total Direct Costs (.60 x $17,366)		10,420.
9.	TOTAL AMOUNT REQUESTED		29,186.

NOTE: The Coral Gables campus negotiated indirect cost rate for the University of Miami for fiscal year 6/1/81 to 5/31/82 is 94.0% of Modified Total Direct Costs (MTDC). The University is willing to accept an indirect cost rate that is lower than the negotiated rate. However, if the proposal is awarded, the University retains the right to exercise any cost clause or cost regulation made a part of the signed agreement.

CURRICULUM VITA

Name: Manuel A. Huerta

Title: Associate Professor of Physi

Date: November 30, 1980

[redacted]

[redacted]

Professional Experience:

Associate Professor of Physics
University of Miami, Coral Gables, Florida
September 1978

Program Associate (on leave from University of Miami)
U.S. - Latin America Cooperative Science Program
National Science Foundation
May 1977 - August 1978

Associate Professor of Physics
University of Miami, Coral Gables, Florida
May 1975 - (Tenured in May 1976)

Assistant Professor of Physics
University of Miami, Coral Gables
September 1972 - May 1975

Associate Research Scientist, Magneto Fluid Dynamics Division
and Adjunct Professor of Mathematics
Courant Institute of Mathematical Sciences, New York University
September 1970 - August 1972

Instructor of Physics
University of Miami, Coral Gables
September 1966 - August 1970

Education:

Ph.D. Physics, January 1970: University of Miami, Coral Gables, Florid
Grade Point Average: 4.0
Dissertation: Approach to Equilibrium of Infinite Chains of Coupled Harmonic Oscillators

M.S. Physics, January 1967: University of Miami, Coral Gables, Florida
Grade Point Average: 4.0

B.S. Electrical Engineering, June 1965: California Institute of Technology, Pasadena, California
Grade Point Average: 3.8
Graduated with Honors

Enrolled at University of Miami in Electrical Engineering from September 1961 to August 1963 then transferred to the California Institute of Technology.
Grade Point Average: 3.8

Scholarships:

NASA Fellowship in Physics, University of Miami, Coral Gables
September 1965 - August 1966.

Graduate Assistant in Physics, Center for Theoretical Studies, University of Miami, Coral Gables
Summer of 1965.

Undergraduate Scholarship, California Institute of Technology
1963 - 1965.

Undergraduate Scholarship, University of Miami, Coral Gables
1962 - 1963.

Honors as Student:

California Institute of Technology's David Joseph McPherson Prize. Awarded upon graduation to the graduating senior in engineering who best exemplified excellence in scholarship.

Membership in Societies:

Tau Beta Pi, Phi Kappa Phi, Sigma Xi, American Physical Society, American Mathematical Society.

Research Fields of Interest:

Plasma Physics, Statistical Mechanics, Solid State Physics, Acoustic Propagation, Nonlinear Partial Differential Equations.

Professional Consulting:

September 1973 - August 1974: Consultant to the Atomic Energy Commission through the Magneto Fluid Dynamics Division of the Courant Institute of Mathematical Sciences of New York University.

Participation in Research Contracts:

September 1973 - August 1974: Principal Investigator in project entitled "Research in Acoustic Propagation and Reflection from Internal Waves" done under a NOAA Grant Number 04-4-022-9.

September 1974 - August 1975: Renewal of above grant.

September 1975 - August 1976: Renewal of above grant.

August 1979 - July 1980: Principal Investigator in Contract Number AFOSR 78-3663 entitled "The Stability and Dynamics of Elastic Structures and Fluid Flows."

July 1980 - July 1981: Principal Investigator in Grant AFOSR 80-0135 entitled, "Analytical Studies of Nonideal Explosives"

Juried Journal Articles

of

Manuel A. Huerta

1. With T.N. Veziroglu, Thermal Conductance of Two Dimensional Eccentric Constrictions; NASA STAR 6, 20, October 23, 1968; STAR Index N-68-32974.

2. With H.S. Robertson, Entropy, Information Theory and the Approach to Equilibrium of Coupled Harmonic Oscillator Systems; J. Stat. Phys. 1, 393 (1969).

3. With H.S. Robertson, Approach to Equilibrium of Coupled Harmonically Bound Systems; Phys. Rev. Letters 23, 825 (1969).

4. With H.S. Robertson, Information Theory and the Approach to Equilibrium; Am. J. Phys. 38 619 (1970).

5. With H.S. Robertson, Entropy Oscillations and the H Theorem for Finite Segments of Infinite Coupled Harmonic Oscillator Chains; Pure and Appl. Chem. 22, 409 (1970).

6. With H.S. Robertson, Approach to Equilibrium of Coupled Harmonic Oscillator Systems II; J. Stat. Phys. 3, 171 (1971).

7. With H.S. Robertson and J.C. Nearing, Exact Equilibration of Harmonically Bound Osbillator Chains; J. Math. Phys. 12, 2305 (1971).

8. With G. Gonzalez, Field Expressions for a Circular Loop Antenna in Terms of a New Set of Functions; J. Appl. Phys. 43, 3975 (1972).

9. With G. Gonzalez, Fresnel Region Fields Produces by Circular Loop and Annular Slot Antennas; J. Appl. Phys. 44, 3500 (1973).

10. With T.N. Veziroglu and S. Kakac, Exact Solutions for Thermal Conductances of Two and Three Dimensional Contacts; Thermal Conductivity 14 (1976), Edited by P.G. Klemens and T.K. Chu, Plenum Publishing Corp., New York, New York.

11. With G.C. Alexandrakis and O.L.S. Lieu, Theory of Nonlinear Phenomena in Ferromagnetic Transmission Resonance; Phys. Rev. B16, 476 (1977).

12. With R.A. Goldstein and J.C. Nearing, Stationary Striations in an Argon Plasma as a Nonlinear Bifurcation Phenomenon; Phys. Fluids, 22 231, (1979).

13. With G. Gonzalez, Surface Potentials of Stratified Spheroidal Volume Conductors Excited by a Current Dipole Source; Int. J. Electronics 47, 213 (1979).

14. With J. Magnan, Spatial Structures in Plasmas with Metastable States as Bifurcation Phenomena; Accepted for publication Phys. Rev. A

15. With G. Gonzalez, The Surface Potentials Produced by Electric Sources in Stratified Spherical and Prolate Spheroidal Volume Conductors; Submitted to IEEE Trans. Biom. Eng.

Other Publications

by

Manuel A. Huerta

1. With J.C. Nearing, W.B. Pardo and M. Reusch, The Interactions of Electromagnetic Radiation with a Forest Environment; subcontract under Lincoln Laboratory of M.I.T., purchase order number C-942 under prime contract number AF 19(628)-5167. Available as a Department of Physics, University of Miami Report, MIAPH-70.10.

2. With J.C. Nearing, W.B. Pardo and M. Reusch, Some Physics of a Florida Forest; Department of Physics, University of Miami Report MIAPH-70.11.

3. Approach to Equilibrium of Infinite Chains of Coupled Harmonic Oscillators; doctoral dissertation, Department of Physics, University of Miami Report MIAPH-69.24.